INTERNATIONAL JOURNAL OF ENERGY STUDIES

Numerical investigation on torque performance of darrieus-savonius hybrid designs

Mehmet Bakırcı*

Department of Mechanical Engineering, Faculty of Engineering, Karabuk University, Karabuk, 78050, Türkiye, ORCID: 0000-0002-1061-698X

*(*Corresponding Author:mehmetbakirci@karabuk.edu.tr)*

Highlights

- The research highlights the potential of hybrid turbines for urban areas and low wind speeds.
- This study provides a comparative analysis of five different turbine (Darrieus, two Darrieus-Darrieus, and two Darrieus-Savonius) designs using 2D unsteady CFD, focusing on torque production and aerodynamic flow characteristics.
- Streamline contours, turbulence intensity profiles, wake flow velocity vectors, and pressure coefficient plots on turbine blades reveal the impact of geometric differences on torque and aerodynamic performance.
- The Darrieus-Savonius hybrid performs better at low TSR but shows reduced efficiency at higher TSR compared to the double Darrieus design.
- None of the designs proposed in this study achieve the torque and power output of the standard Darrieus design at medium and high TSR values.

ABSTRACT

Studies are ongoing on hybrid turbine designs that combine the strengths of Savonius and Darrieus turbines to eliminate their weaknesses and perform efficiently in areas with low and fluctuating wind speeds. This study was conducted to contribute to the development of various hybrid designs and analysis methods in the literature. In this study, two different Darrieus-Darrieus and two different Darrieus-Savonius hybrid turbine designs are proposed with the expectation of achieving better torque and power efficiency. Two-dimensional unsteady RANS CFD analyses have been performed on these turbines. The changes in torque values over time are presented graphically, and the flow characteristics, turbulence intensity, and wake flow have been analyzed. As a result, it has been determined that hybrid designs, while not producing as much power as the standard Darrieus turbine, provide higher torque at low TSR with the nested Darrieus design. The Darrieus-Savonius hybrid produces better torque than the double Darrieus design at low TSR but its performance decreases at high TSR. This study shows that the presented hybrid turbines provide advantages at low TSR but need improvements in terms of power production.
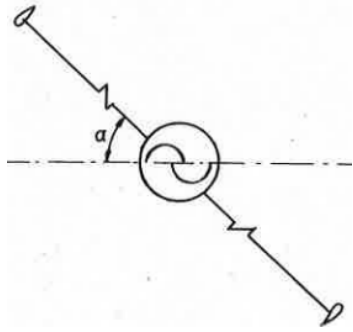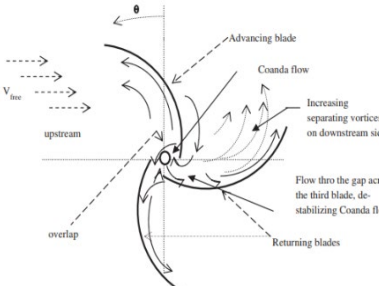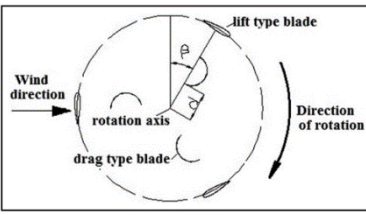
1. INTRODUCTION

Energy is one of the fundamental pillars of the sustainable development of modern societies. The environmental impacts and limited nature of fossil fuels have increased the interest in renewable energy sources to meet the growing energy demand. In this context, wind energy stands out as a clean, reliable, and sustainable energy source. Horizontal axis wind turbines are commonly us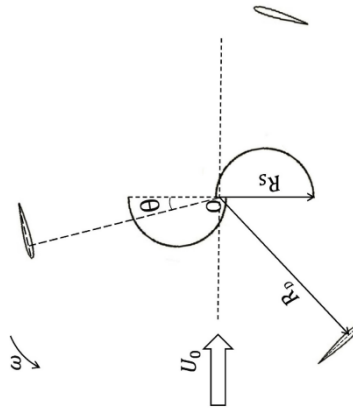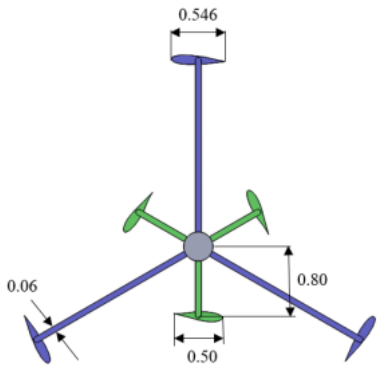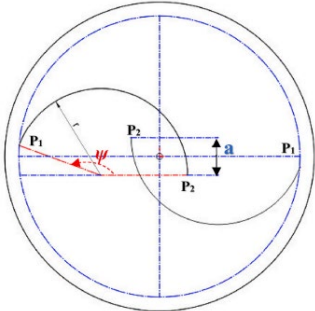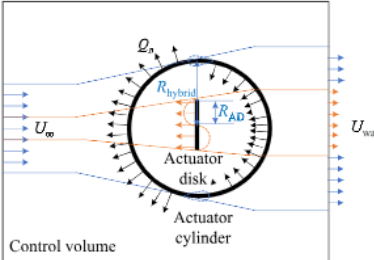ed for electricity generation in environments with high and steady wind speeds. However, in low and variable wind conditions, vertical axis wind turbines can be advantageous in terms of cost, ease of maintenance, and torque generation. Savonius turbines are preferred due to their success in generating torque at low wind speeds and low rotational speeds, as well as their low production and maintenance costs. However, their low power efficiency at medium and high wind speeds and rotational speeds limits their use. On the other hand, although Darrieus turbines do not have as high-power efficiency as horizontal axis turbines, they are significantly more efficient than Savonius turbines. However, they face difficulties in generating torque at low wind and rotational speeds and have poor starting capabilities [1]. For these reasons, hybrid design studies combining the strengths of Savonius and Darrieus turbines have become increasingly important [2-5].

In the literature, various studies have been conducted to improve the performance of Savonius turbines, focusing on topics such as blade numbers [6], blade shapes such as circles, ellips [5], blade combination strategies such as optimum overlap [6], and the use of flow-directing additional apparatuses such as flow deflectors [4, 7, 8]. Similarly, for Darrieus turbines, research has explored different airfoils such as symmetrical and unsymmetrical airfoil selection [9, 10], optimum dimensionless values such as the ratio of airfoil length to rotor radius [11], solidity optimization [10, 12], and the application of fixed or variable pitching angles to the airfoil [11, 13], as well as modifications made to airfoil geometry such as using slat, dimplet, J-shaped [14, 15], H-rotor and helical Darrieus blade shapes [9, 16], and the effect of Reynolds number [13], among other topics [12-24]. A new design study involving the addition of a second, inner Darrieus turbine to a Darrieus rotor was investigated by Muhammad Ahmad [17] using 3D CFD analysis. Additionally, various studies in the literature address the combination of Darrieus and Savonius geometries [2, 3, 5, 17, 18]. In hybrid Darrieus-Savonius turbine designs, topics such as improving starting performance, blade positioning strategies relative to each other [11, 18], and the use of flow-directing additional apparatuses [4, 8, 15] have been explored. Sun et all[19] examined the effect of the relative position of Savonius-Darrieus blades on power performance and observed that the power coefficient (C_P) of the hybrid VAWT was lower than that of the standalone Darrieus rotor.

Table 1 summarize some important studies on Darrieus-savonius hybrid wind turbines.

Table 1. The summary of literature on Darrieus-Savonius studies

The study	Aim-Geometry-Method	Main result (conclusion)	Highlight figure
Gavaldo et al. [18] 1990 "Experimental study on a self-adapting Darrieus–Savonius wind machines"	Darrieus-savonius, Starting torque improvement. Naca0012, R_D=20 cm, R_S=0.35 cm, c(chord)=4 cm, end plates of 15 cm in diameter, overlap=1/6, V=4.5 m/s, Re=1.3*10^5, Experimental-open jet of 30*60 cm in section, pitot tube, dynamometer.	The maximum Cp (power coefficient) for the hybrid turbine (0.35) is lower than that of the Darrieus turbine (0.45). However, the maximum torque coefficient for the hybrid (0.07) is higher than that of the Darrieus (0.02).	
Gupta et al. [25] 2008 "Comparative study of a three-bucket Savonius rotor with a combined three-bucket Savonius–three-bladed Darrieus rotor"	A combination with a three-bladed Savonius turbine at the top and a three-bladed Darrieus turbine at the bottom could leverage the unique strengths of each type. Here, each Savonius blade spans a 150° arc, and the setup has an 8 cm diameter.	While the overlap increases the Cp value in standard Savonius designs, it decreases in hybrid designs. This is explained by the "Coanda effect." In hybrid designs with a three-bladed Darrieus-Savonius configuration, overlap should not be used, especially at medium and high speeds.	
Sun et al. [19] 2016 "Research on the aerodynamic characteristics of a lift drag hybrid vertical axis wind turbine"	Inner circular arcs for drag, outer airfoils for lift. Circle diameter=50m, distance from center d=15 cm, chord length c=50 cm, Darrieus diameter=3 m. Effect of Aspect Ratio (H/c).	In cases with high Aspect Ratio (AR) values, 2D CFD results for the power coefficient (Cp) are more accurate, while at low AR values, Cp values obtained from 2D CFD tend to be overestimated compared to actual values.	
Liang et al. [13] 2017 "A computational study of the effects of the radius ratio and attachment angle on the performance of a Darrieus-Savonius combined wind turbine"	Nested Darrieus-Savonius hybrid design. R_D = 75 cm, overlap e/D = 0.1, Naca 0012, Chord, c =22 cm. Optimization of the angle (θ), Savonius radius (R_S), Darrieus blade number, and solidity for optimal values. Solidity is calculated as Solidity ($=Nc/2R_D$). Wind speed V=3 m/s. CFD analysis using the realizable $k-\epsilon$ turbulence model.	The maximum Cp value for a standard Darrieus turbine is calculated as 0.32. For the hybrid design with two Darrieus blades, Rs/R_D=1/4, and θ=0 degrees, the maximum Cp value achieved is 0.363. When the solidity reaches 0.293, the maximum Cp value increases further to 0.397.	

Ahmed et all [17] 2022 "Design optimization of Double-Darrieus hybrid vertical axis wind turbine"	Two Darrieus rotors, each with three blades, are nested. The airfoil used is NACA 0018. The radius and chord lengths, heights, and pitch angles of both the inner and outer rotors are optimized using DOE (Design of Experiments), RSM (Response Surface Methodology), and 3D unsteady CFD analysis.	First, the optimized values for the inner rotor are obtained: R=0.789 m, H=1.605 m. Then, the optimal dimensions for the outer rotor are determined: D=3.854 m, H=3.12 m, c=0.547 m, and pitch angle; Θ=-3.41˚.	
Abdelaziz et all [27] 2024 "Performance investigation of a Savonius rotor by varying the blade arc angles"	For a Savonius blade with 2 blades and a circular diameter of 18 cm, optimize the blade shape and the relative positioning of the circular arcs. Determine the optimal overlap ratio and arc degree, within a range of 140˚ to 190˚.	The maximum Cp value of 1.983 was achieved at a TSR of 0.8 with an overlap ratio of 0.2 and a circular arc 180˚, along with an optimized blade geometry. This Cp value is 12.9% higher compared to the conventional Savonius design.	
Pan et all [3] 2024 "Performance analysis of an idealized Darrieus–Savonius combined vertical axis wind turbine"	To investigate the power performance of the idealized hybrid VAWT, the actuator disk and cylinder models are implemented in OpenFOAM.	Hybrid designs, while providing higher torque at low TSR, cannot achieve a significant increase in power production compared to traditional Darrieus turbines by altering operational and geometric conditions.	

In the literature, studies typically focus on a single hybrid design, whereas this study examines the performance of multiple designs within a single study. Five different wind turbine designs are presented, including a standard Darrieus turbine, two different nested Darrieus hybrids, and two different Darrieus-Savonius hybrids. Two-dimensional unsteady CFD analyses were conducted for these turbines. As a result of the CFD analyses, streamline contours were obtained to observe the effects of blade geometries on the flow, torque-time graphs were analyzed to explore how the produced torque changes over time, turbulence intensity contours were generated to identify regions where flow fluctuations are concentrated, and wake velocity profiles were produced to determine the optimal distance between the two turbines. The results obtained were comparatively evaluated and interpreted for four different TSR values and five different geometries. The most

significant outcome of the study was to reveal how the average torque values obtained at different TSR values varied among the five different geometries.

This current study makes a significant contribution to the body of knowledge in the literature by highlighting the potential of different design configurations to improve wind turbine efficiency. The contribution of the study lies in the analysis of five different designs instead of a single hybrid turbine design. While the literature generally contains analyses based on a single design, this study offers a novelty by directly comparing the performances of different hybrid configurations. Another contribution of this study to the literature is the comparison of various turbine designs in terms of torque and power production, elucidating the performance differences between hybrid and standard designs. With its innovative approach and comprehensive comparison method, this research serves as an important resource for the development of wind energy technologies in both academic and practical fields.

2. METHODOLOGY

The mathematical equations used in this study, the two-dimensional design geometries of the proposed new hybrid vertical axis wind turbine designs, and the computational fluid dynamics used for their aerodynamic analyses were explained sequentially.

The basic equations [17] related to the vertical wind turbine power can be given as follows: The maximum power (P_{max}) from the wind passing through a vertical axis wind turbine with an area A can be calculated using Equation 1.

$$P_{max} = \frac{1}{2}\rho A V^3 \tag{1}$$

$$A = DH \tag{2}$$

ρ, A, D, H, V are air density, area, diameter, height, wind velocity respectively. And the angular velocity(ω) of the turbine and TSR can be calculated with the following equations [1]:

$$\omega = \frac{2\pi N}{60} \tag{3}$$

Where *N* is revolution number per minutes. Tip speed ratio is defined as the ratio of the blade's tip speed to wind velocity.

$$TSR = \frac{\omega r}{V} \tag{4}$$

Available power (P_a) is calculated by product of average torque(*Q*) value and angular velocity(ω).

$$P_a = Q\omega \tag{5}$$

The power coefficient of the wind turbine (*Cp*) can be calculated using the Equation 6:

$$C_P = \frac{P_a}{P_{max}} \tag{6}$$

Average torque is calculated by Equation 7;

$$Q = \frac{1}{T}\int_0^T Q(t)dt \tag{7}$$

Where *Q* is torque (Nm), T is peryot(s), t is time(s). Pressure coefficient(*CP*) is defined as;

$$CP = \frac{P - P_0}{\frac{1}{2}\rho V^2} \tag{8}$$

Where *P* is static pressure, *P₀* is atmospheric pressure, *V* is free stream velocity of the flow. Instanteonous torque coefficient C_Q is calculated by using Equation 9;

$$C_Q = \frac{Q}{\frac{1}{2}\rho V^2 (DH)R} \tag{9}$$

A total of five different designs were presented: one standard Darrieus (A), two different Darrieus-Darrieus hybrids (B and C), and two different Darrieus-Savonius hybrids (D and E). The Savonius geometry was created with three 120-degree arc-shaped blades symmetrically joined at the center.

In this study, the effects of the central shaft on the flow were not considered and overlap situations where the blade connection points converge at a single point were not examined. Previous studies in the literature have analyzed various versions of these geometries and the effects of their assembly strategies on power performance yielding significant findings. Similarly, the impact of parameters such as the ratio of airfoil length to rotor radius, the use of symmetric and asymmetric airfoils, and fixed or variable pitching angles on the power performance of Darrieus turbine geometries have been explored. However, this study focuses solely on uncovering the differences in torque production performance among the five different designs (A, B, C, D, E). Therefore, without delving into detailed designs and various variables in the literature, the effects of only the basic geometric differences were addressed. For the two-dimensional Darrieus turbine geometry, the rotor diameter was set at 1030 mm, with 3 blades, a blade profile of NACA 0021, and an airfoil chord length of 85.8 mm. These five different designs are shown in Figure 1.
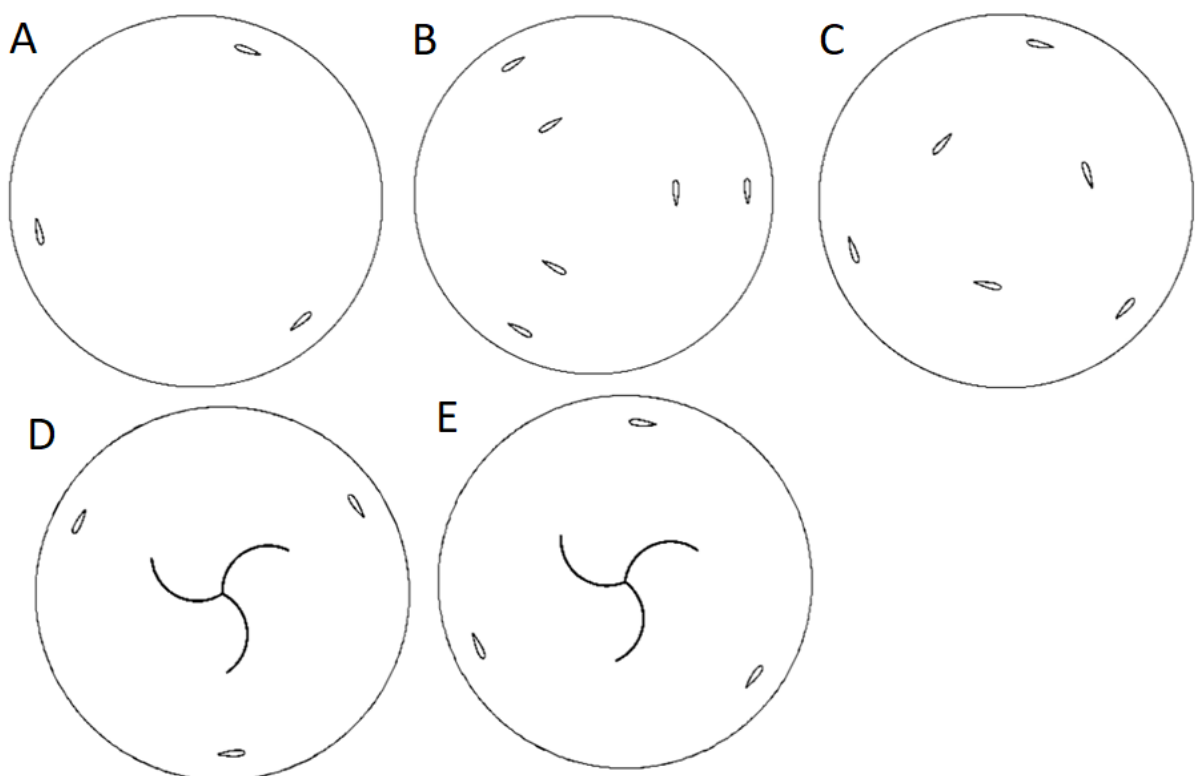
Figure 1. Five different designs

In Savonius turbines, theoretical calculations are based on the net values of positive and negative drag forces acting on concave and convex surfaces. These calculations are made based on the drag forces acting on the arc-shaped blades, the drag coefficients, and the net torque values transmitted

to the central shaft. In Darrieus turbines, using the double stream tube model, the lift forces, drag forces acting on the blades, and the torque values generated according to their azimuth angles are calculated. However, for hybrid turbines, these theoretical models need to be modified due to the more complex geometries and aerodynamic structures that combine both turbines. While calculating such complex structures is quite difficult and limited with theoretical methods, these analyses can be easily performed using CFD methods.

The necessity of using CFD for detailed flow analyses of hybrid designs is highlighted in this study. Hybrid designs formed by the combination of Savonius and Darrieus turbines cannot be accurately analyzed with theoretical models due to complex flow structures and interactions between the blades. CFD can more easily perform flow analysis of such complex geometries and simulate detailed aerodynamic phenomena such as vortex structures around the blades, streamlines, and flow separations. Especially in hybrid turbines that combine the drag-based calculations of Savonius blades and the lift force with torque production processes of Darrieus blades, the flexibility of CFD comes into play in cases where these theoretical models fall short. To understand the performance of hybrid turbine designs, theoretical calculations alone are insufficient, as these calculations are typically limited by simplified assumptions.

In this study, there is a need to measure the performance of five different hybrid turbine designs at four different TSR (tip speed ratio) values and visualize the flow. This goes beyond the limits of theoretical and experimental methods. While experimental methods may be preferred for analyzing a single design at a constant wind speed and a specific TSR value, when multiple designs and a wide range of parameters need to be tested, experimental studies become both costly and time-consuming. The processes such as prototype production for each of the five different designs and flow visualization using PIV (Particle Image Velocimetry) techniques make experimental studies quite challenging and expensive. CFD methods allow for the simultaneous analysis of all these designs while enabling rapid and detailed performance measurements for different wind speeds and TSR values. Therefore, in this study, the CFD method was chosen, providing a much more efficient and applicable solution for the analysis of hybrid turbines compared to theoretical and experimental methods.

In this study, an unsteady two-dimensional CFD analysis was conducted to examine the aerodynamic performance of turbine designs. The analyses were performed using a two-

dimensional unsteady RANS model, which may limit the accuracy of the results due to constraints in fully simulating three-dimensional flow and turbulence effects. In cases with high Aspect Ratio (AR=H/c) values, 2D CFD results for Cp are more accurate, while at low AR values, Cp values obtained from 2D CFD tend to be overestimated compared to actual values [3]. However, this approach has provided a quick and effective means of comparing the performance between different designs. The wind speed was adjusted to 9 m/s, and four different TSR values (1.43, 2.51, 3.29, and 4) were used. These measurements and values were taken from Castelli's 2011 study [20], allowing for verification and validation processes to be carried out.

In unsteady CFD analyses, the dynamic torque obtained from the Darrieus turbine takes on different values at each rotation angle of the turbine. This is particularly important due to the operating principle of Darrieus turbines, as these turbines generate torque by creating lift as the blades interact with the wind. In Darrieus turbines, the angle of attack created by the airfoils with the wind continuously changes due to the rotational movement. This variation causes the torque value to fluctuate periodically over time. Unsteady CFD simulations are conducted to analyze this fluctuation. These simulations step-by-step solve the turbine's operating conditions and the flow of wind over time. Thus, the changes in torque at every moment can be detailed. Dynamic torque data is critical for understanding turbine performance and optimizing it. The average torque is calculated by integrating over time, and this average value is used to determine the mechanical power output of the turbine [21].

The analyses of hybrid designs have generally been conducted in the literature using CFD and experimental methods. In the literature, studies have focused on dimensionless parameters such as radius, airfoil length, and solidity to determine the optimal geometry in hybrid designs. Most of these studies have been carried out using 2D unsteady CFD solutions, with some validated against experimental data. Additionally, there are more advanced analyses in the literature, such as Large Eddy Simulation (LES) and Detached Eddy Simulation (DES), applied for 3D solutions. In applied CFD studies, turbulence models such as Spalart-Allmaras, standard, realizable, k-epsilon, and k-omega are typically used, with the SST k-omega model being the most preferred [21]. In this study, the SST k-omega model was also employed for 2D unsteady RANS analyses. The main aim of the study was to compare the torque performance of different two-dimensional combinations of Darrieus and Savonius geometries, and successful solutions obtained indicated that there was no need for 3D analyses.

To obtain accurate and reliable results during the analysis process, the quality of the mesh, time step size, iterations per step, boundary conditions, and other critical parameters have been meticulously optimized. A mesh convergence study was conducted by reducing the mesh in multiples of $\sqrt{2}$ to understand the accuracy of the mesh resolution. The orthogonality value was kept close to 1, the skewness value near zero, and the aspect ratio was ensured to be less than 10. Approximately 90% of the mesh had an aspect ratio close to 1. It has been experienced that the results of inflation optimization significantly affect the mesh quality. Maintaining the Y+ value close to 1 is critical for boundary layer resolution, so this value was adjusted to be around 1. Additionally, the time step size was adjusted accordingly to keep the Courant-Friedrichs-Lewy (CFL) number around 1, as having a CFL number near 1 is another important criterion that enhances the numerical accuracy of the solution. The mesh, Y+, and CFL factors were optimized until the values closest to the experimental results were achieved. The boundary conditions were defined as they were in the experiment [20]. A velocity boundary condition was applied in the inlet region, while zero-gauge pressure was applied in the outlet region. The side walls, turbine blade surfaces, and rotor shaft were defined as no-slip walls. The unstable condition encountered at the beginning of the solution was disregarded, and only the data obtained during the iterative stability period, where convergence was observed, were considered. Proper adjustment of all these factors ensured that the CFD results were consistent and reliable compared to other studies in the literature.

The dimensions of the rectangular flow domain are a length of 7.75 m, a width of 3.75 m, a pre-flow region length of 2.5 m, a post-flow region length of 5.25 m, and a rotating rotor diameter of 1.25 m, as shown in Figure 2. The rotor area is defined as a rotational mesh, and the sliding mesh method is used in the simulation [20].

The total number of meshes used in the flow field is 717593. Mesh quality is particularly important around the airfoil, and the mesh representation at the airfoil's trailing edge is shown in Figure 3.
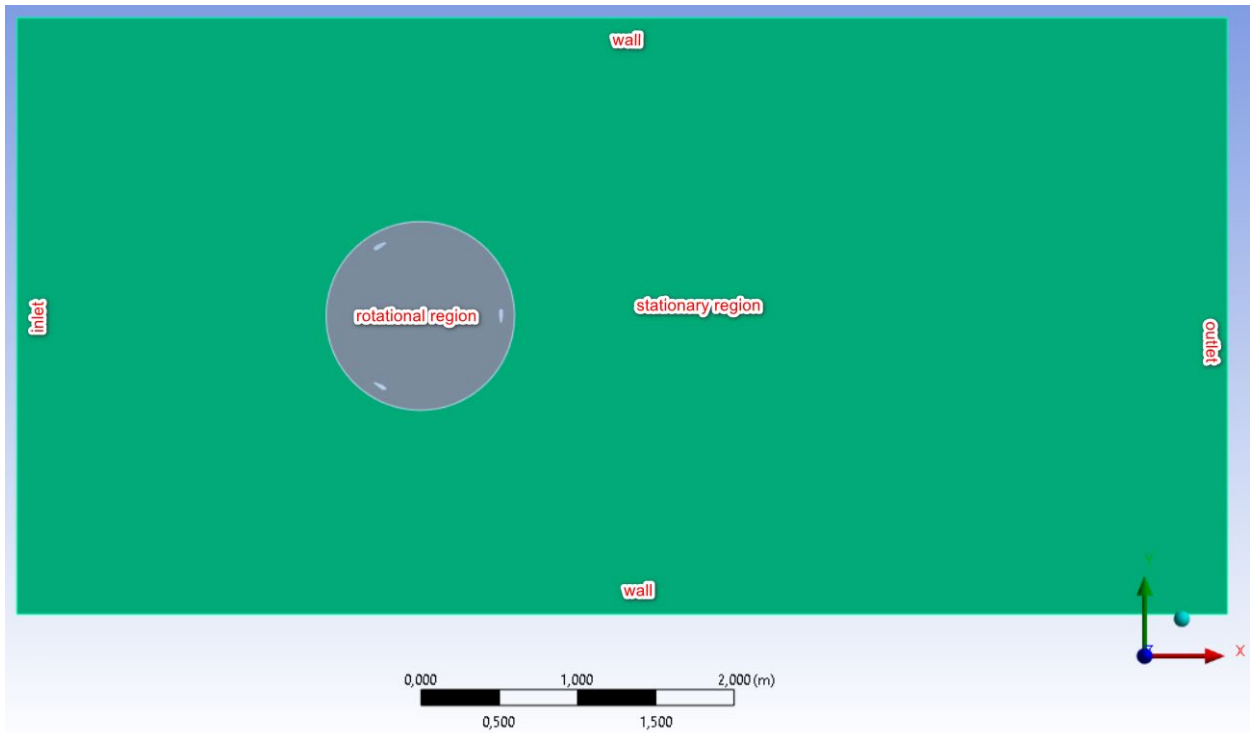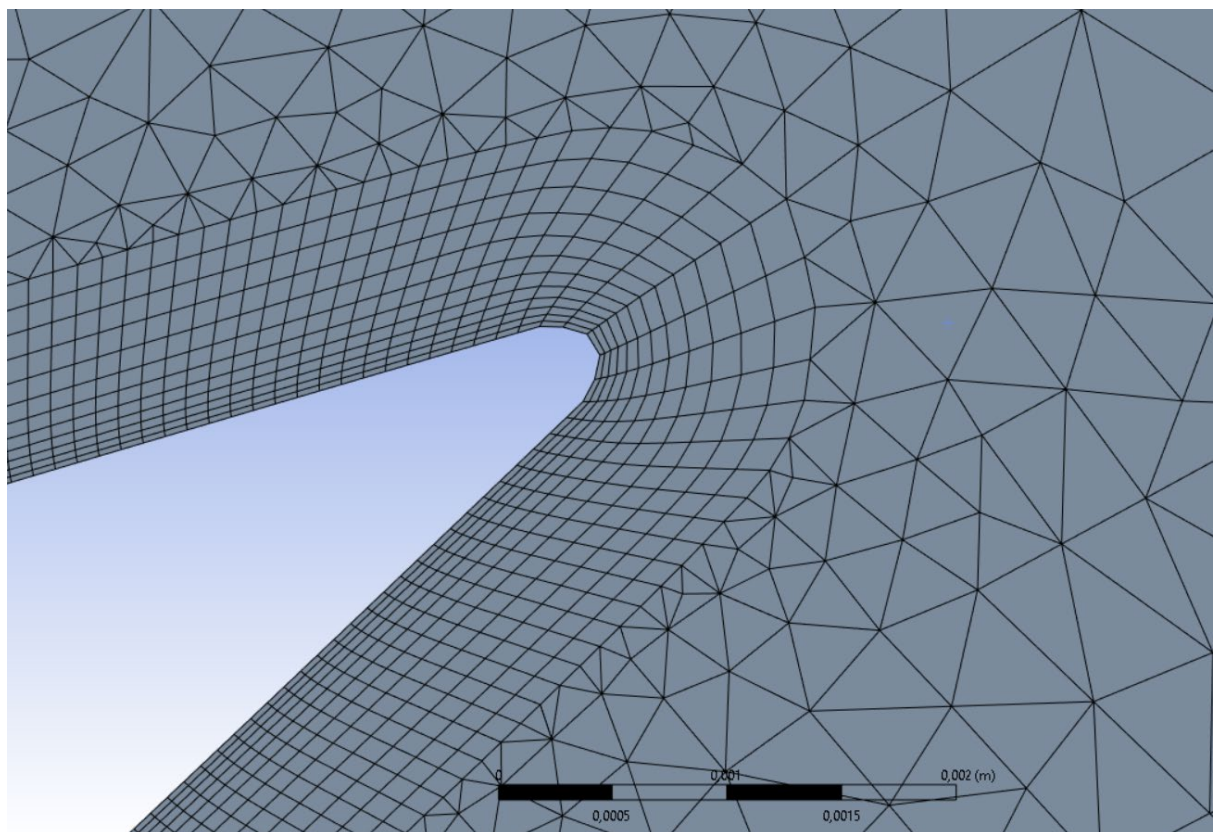
Figure 2. Fluid domain

Figure 3. The mesh representation at the airfoil's trailing edge.

647

3. RESULTS AND DISCUSSION

The pressure coefficient contours, time-varying torque graphs, flow field streamlines, turbulence intensity contours, and wake velocity profiles were obtained from the CFD analyses of the Standard Darrieus (Design A) and hybrid designs (Designs B, C, D, and E) at TSR values of 1.43, 2.51, 3.29, and 4. These results were evaluated in terms of the torque production efficiency of the turbines and flow characteristics.

Design A: While the Standard Darrieus (Design A) blades rotate, the pressure coefficient (*CP*) graphs formed on the airfoil at different positions (azimuth angles) were obtained for four different TSR values. For example, at a TSR value of 2.51, the *CP* graphs obtained at 0° and 180° azimuth angle positions are shown in Figure 4.
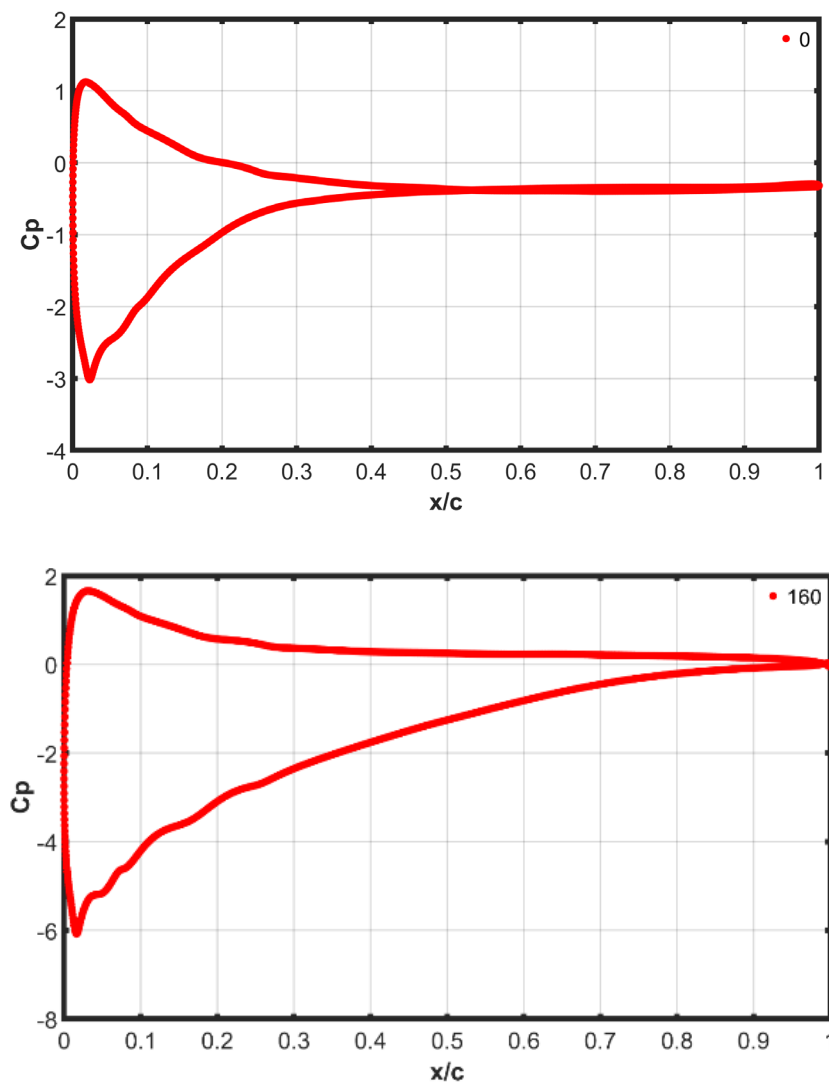
Figure 4. Pressure coefficient (*CP*) graphs of Design A

While the minimum *CP* value at 0° is -3, this value increases to -6 at the 180° position. These negative values indicate a strong suction force on the airfoil's suction side. The area enclosed by the graphs represents the magnitude of the lift force on the airfoil. It can be seen from the graph that the lift force at the 180° position is greater than that at the 0° position. As examples of the variations in torque values over time for Design A (Standard Darrieus), the graphs obtained at TSR values of 1.43 and 4 were presented in Figure 5.
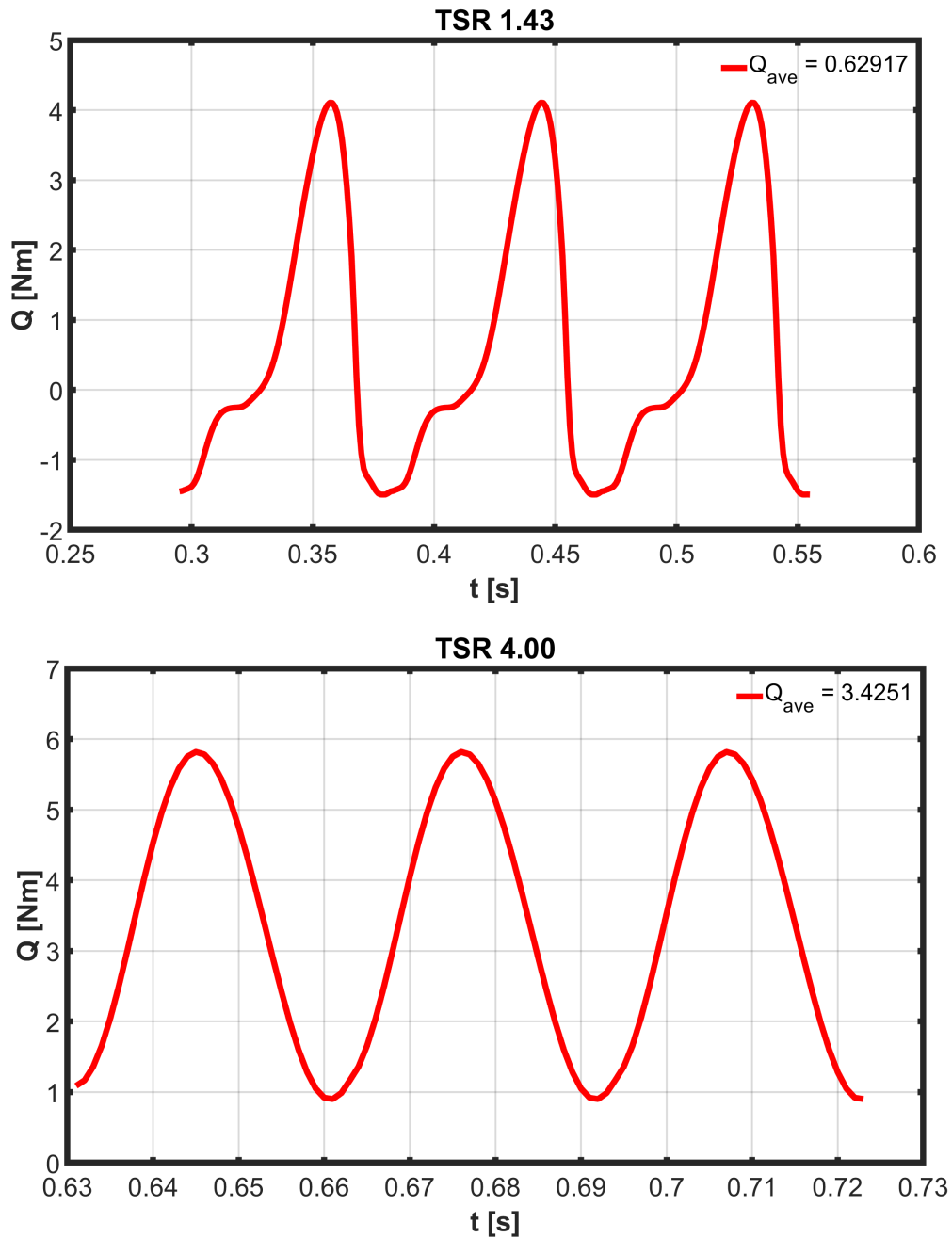
Figure 5. Torque graphs of Design A for TSR of 1.43 and 4.00 values

In the graph for TSR of 1.43, the maximum torque value is 4.1 Nm, the minimum value is -1.4 Nm, and the average value is 0.629 Nm. For the case where TSR is 4, these values are 6 Nm, 1 Nm, and 3.425 Nm, respectively. Streamlines are among the most important graphs that illustrate the structure of the flow. The turbulence intensity contours show the distribution of fluctuations in flow velocity within the flow region. The velocity streamlines and turbulence intensity contours obtained at the shown position for a TSR value of 2.51 for the Standard Darrieus were illustrated in Figure 6.

The streamline contour can illustrate how the fluid flowing from one blade affects the flow approaching the other blade, as shown in the figure. In the figure, one blade (at 0° position) remains unaffected, while the blade in the wind inlet region (at 120° position) influences the blade located further back (at 240° position). The turbulence intensity shown in the figure is primarily observed at the airfoil's trailing edge and in the wake, with a maximum value of 4.67%. It is clear from the contour that the maximum values are found at the airfoil's trailing edge, while relatively larger values occur along the airfoil's wake. Analyzing the wake flows of wind turbines is important for various reasons. For instance, it can determine how far downstream the disturbed or decelerated flow recovers, which helps establish the minimum spacing required between consecutive turbines. The variation of average torque values for the Standard Darrieus design at four different TSR values was illustrated in Figure 7.

Velocity profiles were obtained for the Standard Darrieus at a TSR of 2.51 at positions where the x distances are 1 m, 2 m, and 3 m. Based on these velocity profiles, we can say that the flow recovers to its original state approximately 3 m downstream from the center of the turbine with a diameter of about 1 m. As shown in Figure 7, the highest average torque value was obtained at a TSR of 2.51.

Design B: A new design (B) was created by adding second blades with the same center but a smaller radius to the blades of the Standard Darrieus turbine. The aim of this design is to achieve higher torque at low TSR values. Pressure coefficient graphs were obtained for different positions (azimuth angles) of the airfoil taken at 40° intervals from 0° to 360°. These graphs for the inner and outer airfoils were compared. The *CP* graphs for the 160° and 320° positions are shown in Figure 8 as two examples.
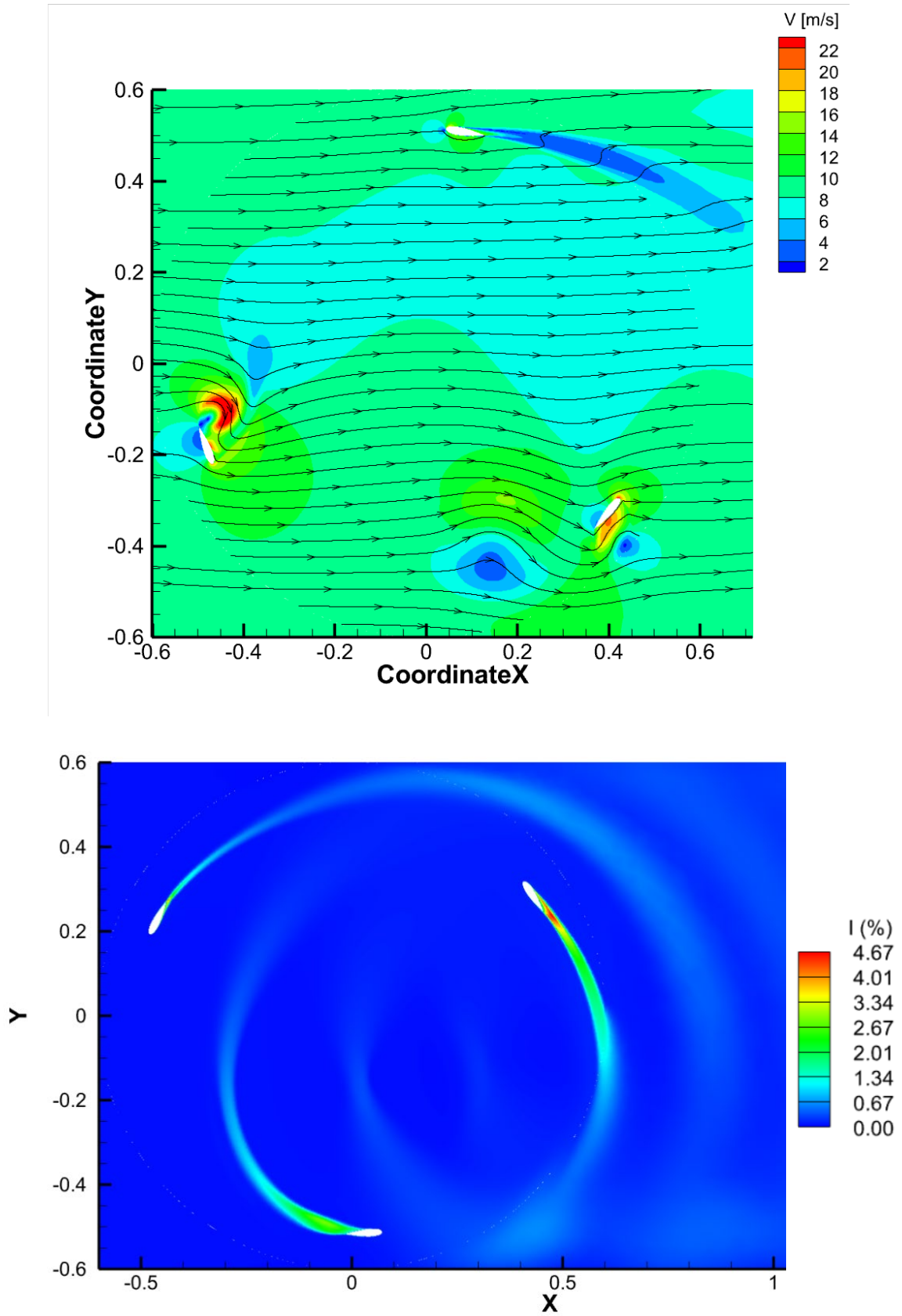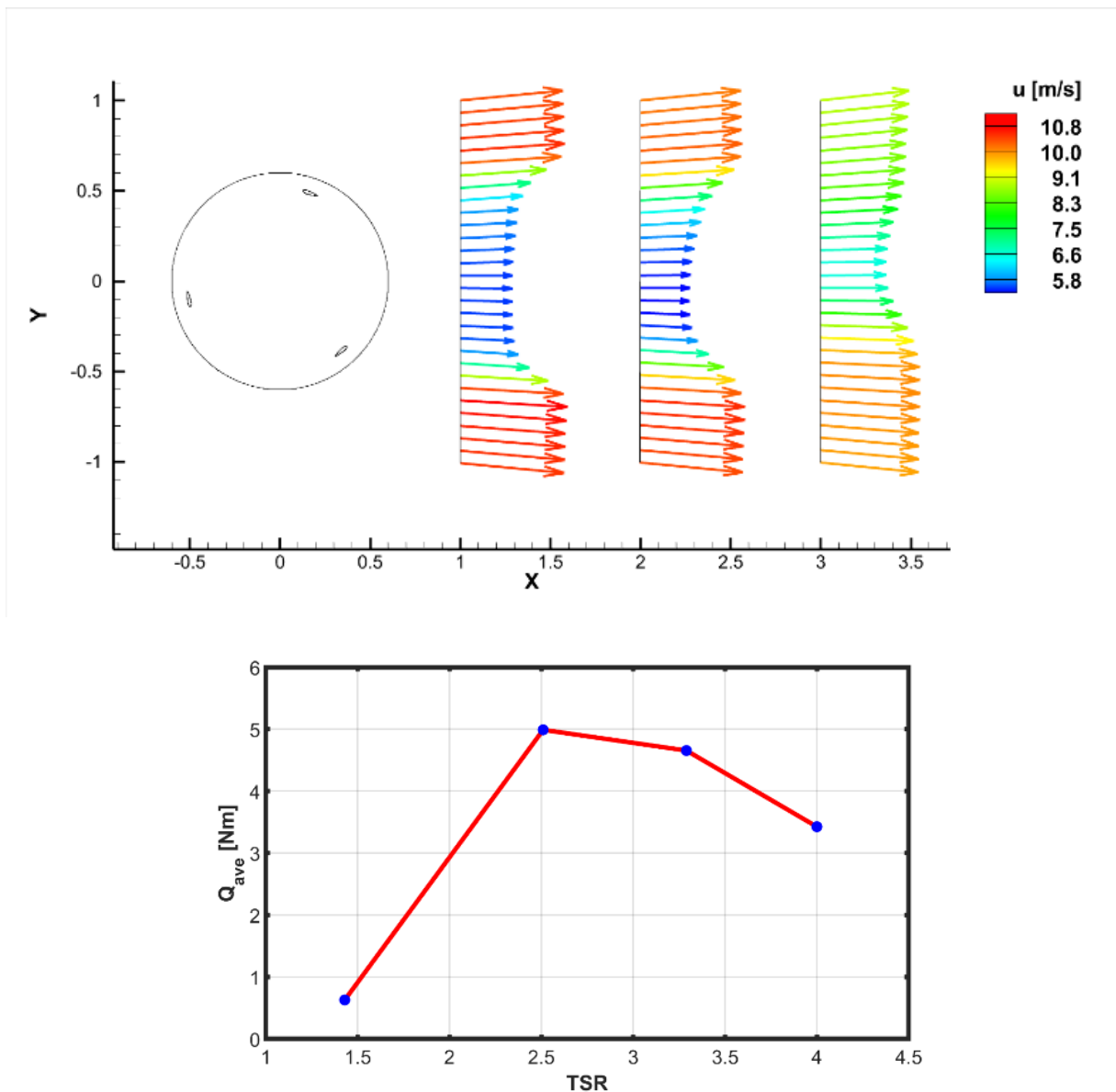
Figure 6. Streamlines and turbulence intensity contours for Design A

Figure 7. The variation of the velocity profile and average torque values of Design A

At the 160° position, a larger lift force is generated on the outer airfoil, while at the 320° position, a larger lift force is produced on the inner airfoil. It can also be observed that the total lift force at 160° is greater than that at 320°. In the first case, the *CP* value ranges from -8 to 2, while in the second case, it ranges from -0.8 to 2.7. When examining the *CP* graphs for all positions, it has been determined that higher lift forces are generally generated on the outer airfoils. Torque variation graphs over time have been obtained based on the analysis results of the Double Darrieus design at four different TSR values. The results for TSR values of 1.43 and 2.51 are presented in Figure 9.

At a TSR value of 1.43, the torque values range from -3.2 to 5, with an average value of 0.681 Nm. At a TSR value of 2.51, the minimum torque value is approximately -0.8 Nm, the maximum value is 10 Nm, and the average value is 4.167 Nm.

Streamline contours in the flow field at different positions have been obtained, one of which, related to TSR 2.51, is shown in Figure 10. When two parallel airfoils are too close to each other, we can predict that the flow will lose its smoothness, resulting in insufficient lift force on the airfoil. Part of the flow approaching the airfoil passes underneath, while another part passes above it. The flow that passes above accelerates, causing the static pressure to drop according to Bernoulli's principle. The pressure difference created on both sides of the airfoil generates lift, which in turn produces the tangential force responsible for torque. It can be observed in the contour that the speed, which is 9 m/s in the free region, increases due to the turbine effect, reaching a maximum value of 48.7 m/s.

The turbulence intensity distribution and maximum value generated in the flow field were examined at different TSR values and positions. Turbulence intensity expresses the density of velocity fluctuations in the flow. The turbulence intensity contour for the double design (B) at a TSR value of 2.51 is shown in the figure. The maximum turbulence intensity value was 4.25%. In Figure 10, as the blades pass around the 140° position, the outer airfoil produces particularly high turbulence intensity at its trailing edge.

Looking at the velocity profiles in the wake of design B, it is understood that the flow does not completely return to its original state at the position x=3 m. In design A, however, the flow was able to return to its original condition at the same position. Unlike design A, it can be said that in the velocity profiles shown for design B, the flow progresses with vertical direction changes. The graph of average torque values obtained at TSR values of 1.43, 2.51, 3.29, and 4 for design B is shown in Figure 11.

Stabilizing torque fluctuations in Darrieus turbines is critical for performance and structural integrity. Analyzing torque variation within one rotation cycle involves evaluating the maximum, minimum, and average torque values. If maximum and minimum torque values are close to the average, torque stability improves, reducing mechanical stress and maintaining power quality. Torque stability is quantified using the formula;

$$\beta = \frac{Q_{max} - Q_{min}}{Q_{average}} \qquad (10)$$

where a lower β value indicates greater stability. High stability minimizes deformation and material stress on turbine blades, enhancing turbine longevity and efficiency.
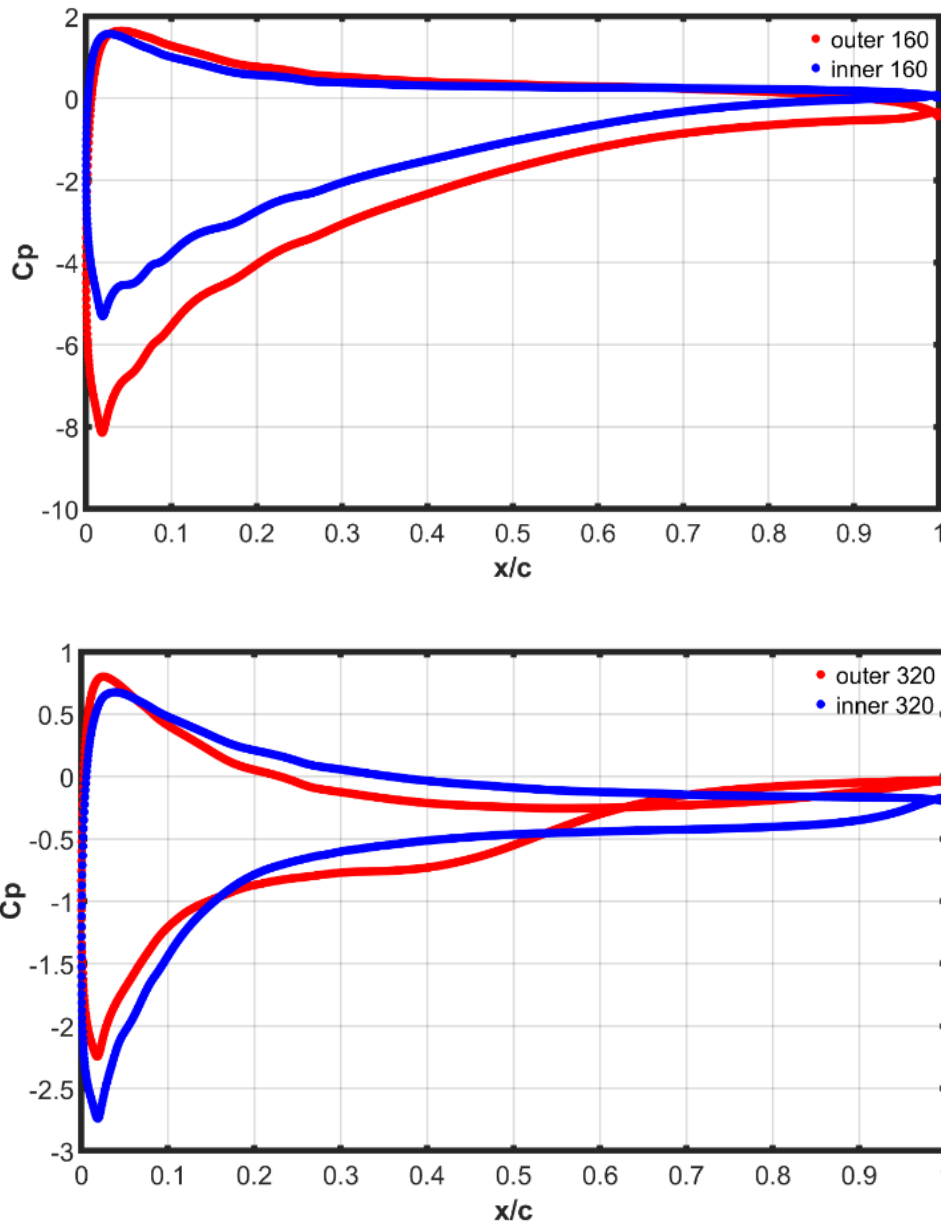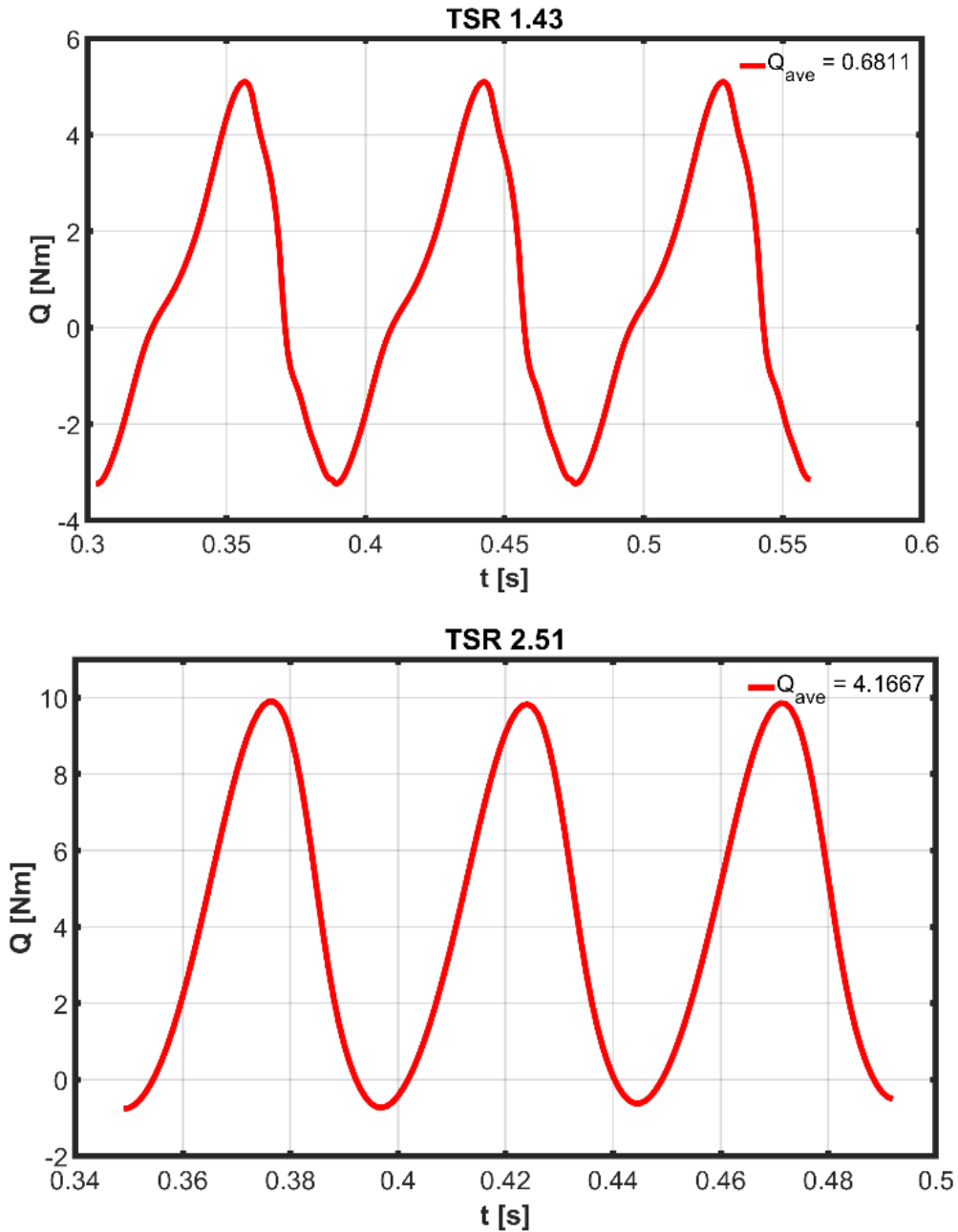

Figure 8. Pressure coefficient (*CP*) graphs of Design B

Figure 9. Torque graphs of Design B for TSR 1.43 and 4.00

The β value is approximately 12.3 at a TSR of 1.43, while it decreases to around 2.64 at a TSR of 2.51. At a TSR of 2.51, not only is more torque generated, but the torque is also more stable. This stability is advantageous for both structural strength and vibration reduction, as well as for maintaining high power quality.
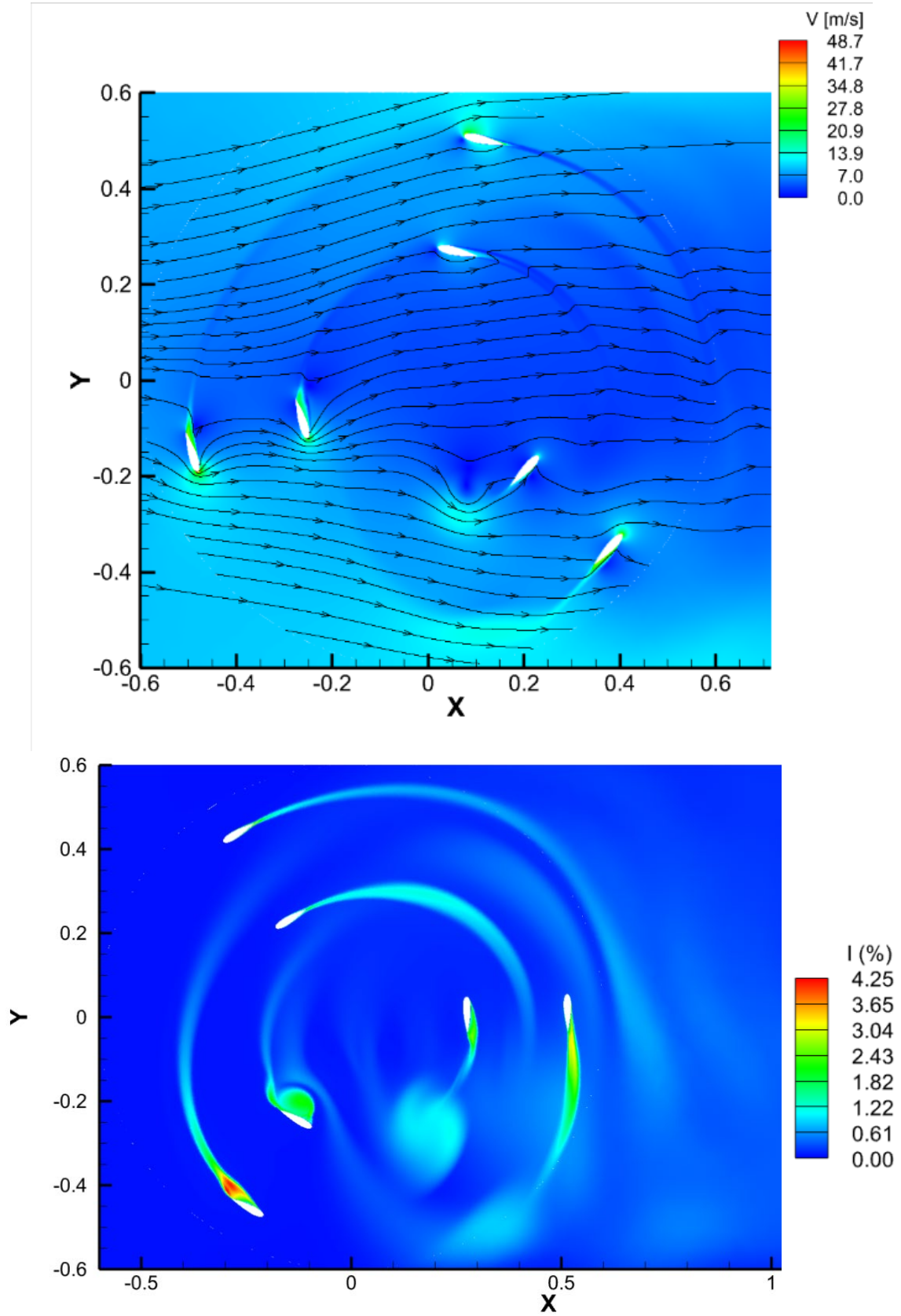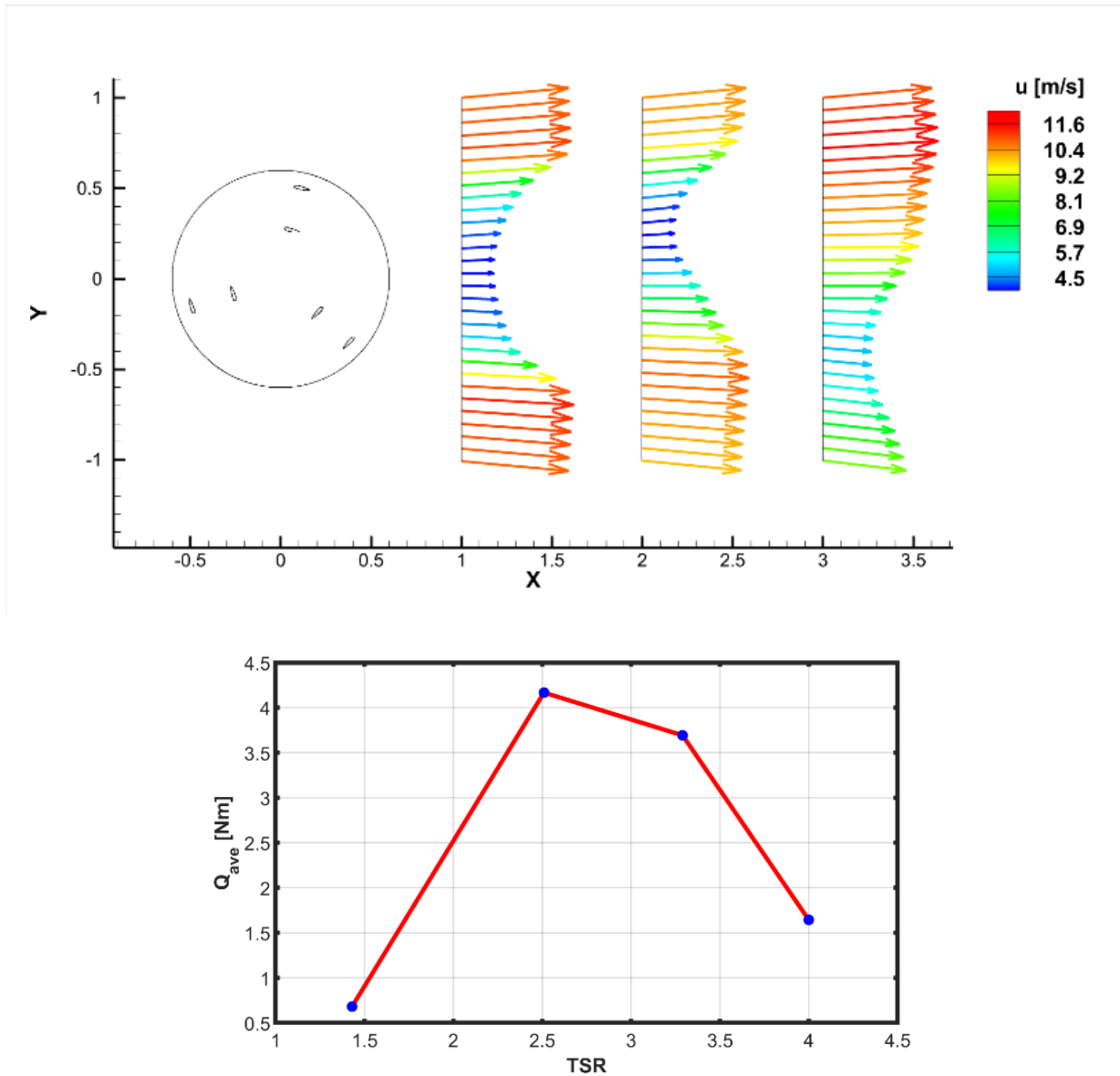
**Figure 10.** Streamlines and turbulence intensity contours for Design B

Figure 11. The variation of the velocity profiles and average torque values of Design B

The highest torque value was achieved at a TSR of 2.51, like Design A (Figure 11). The average torque value obtained at a TSR of 1.43 in Design B was higher than that in Design A. However, at other TSR values, Design B produced relatively lower torque compared to Design A. This situation can be seen as a success for Design B at lower TSR values, even though it generates lower torque values at higher TSR values.

Design C: Design C is like Design B, but a 60° offset was applied between the inner and outer blades. *CP* graphs were obtained for Design C. At a TSR of 2.51, graphs obtained at nine different

positions are presented, with two of them shown in the figure. By examining these graphs, it is possible to interpret the lift forces generated on the airfoil.
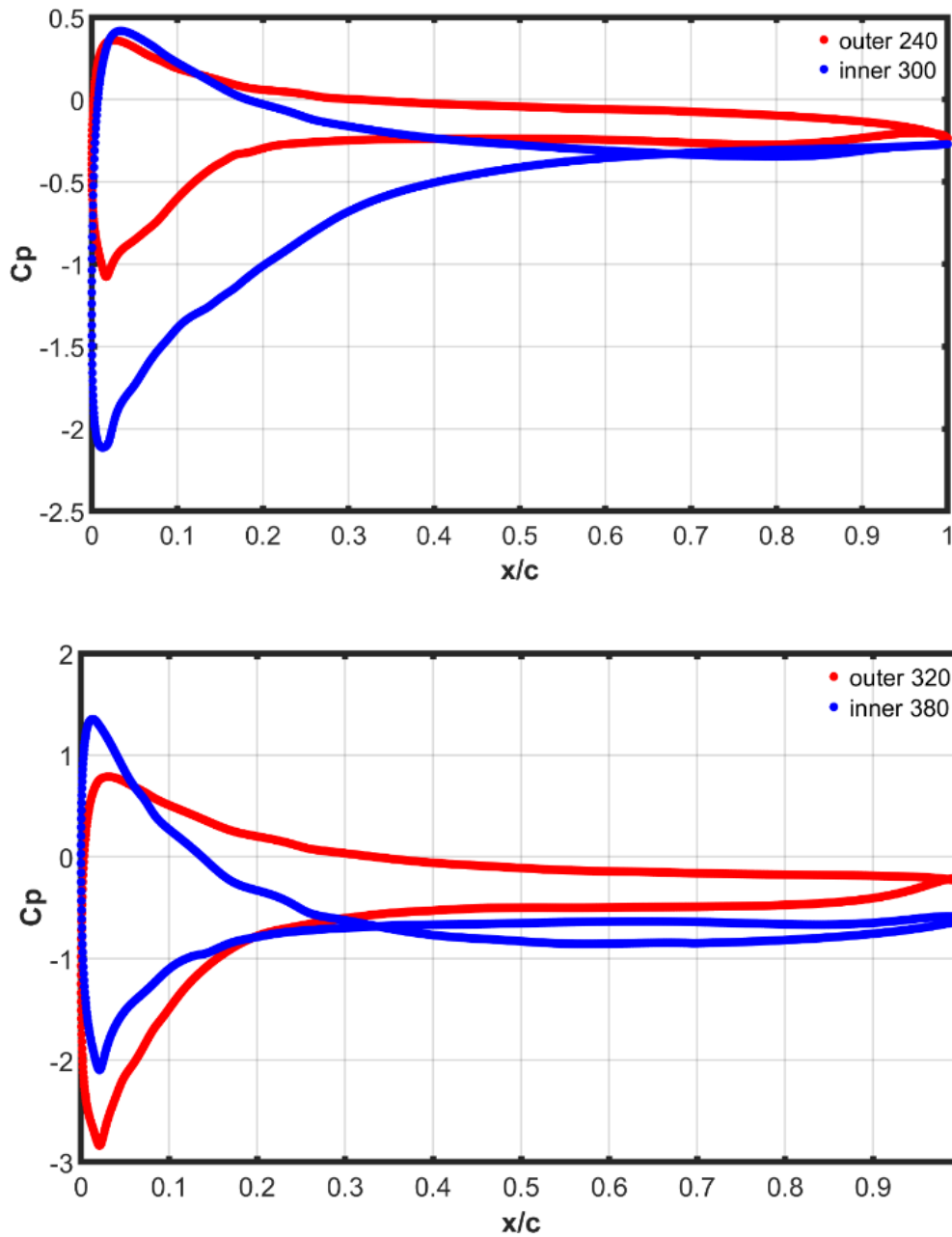
Figure 12. Pressure coefficient (*CP)* graphs of Design C

The *CP* graphs generated on the outer blade and inner blade can be compared; at the 240° position, better lift is produced on the inner blade, while at the 320° position, better lift is produced on the outer blade. These results and interpretations will provide insights into what changes can be made in the design to achieve improvements. The variation of torque produced by Design C at TSR=1.43 and TSR=2.51 over time (or azimuth angle - position) is illustrated in Figure 12.
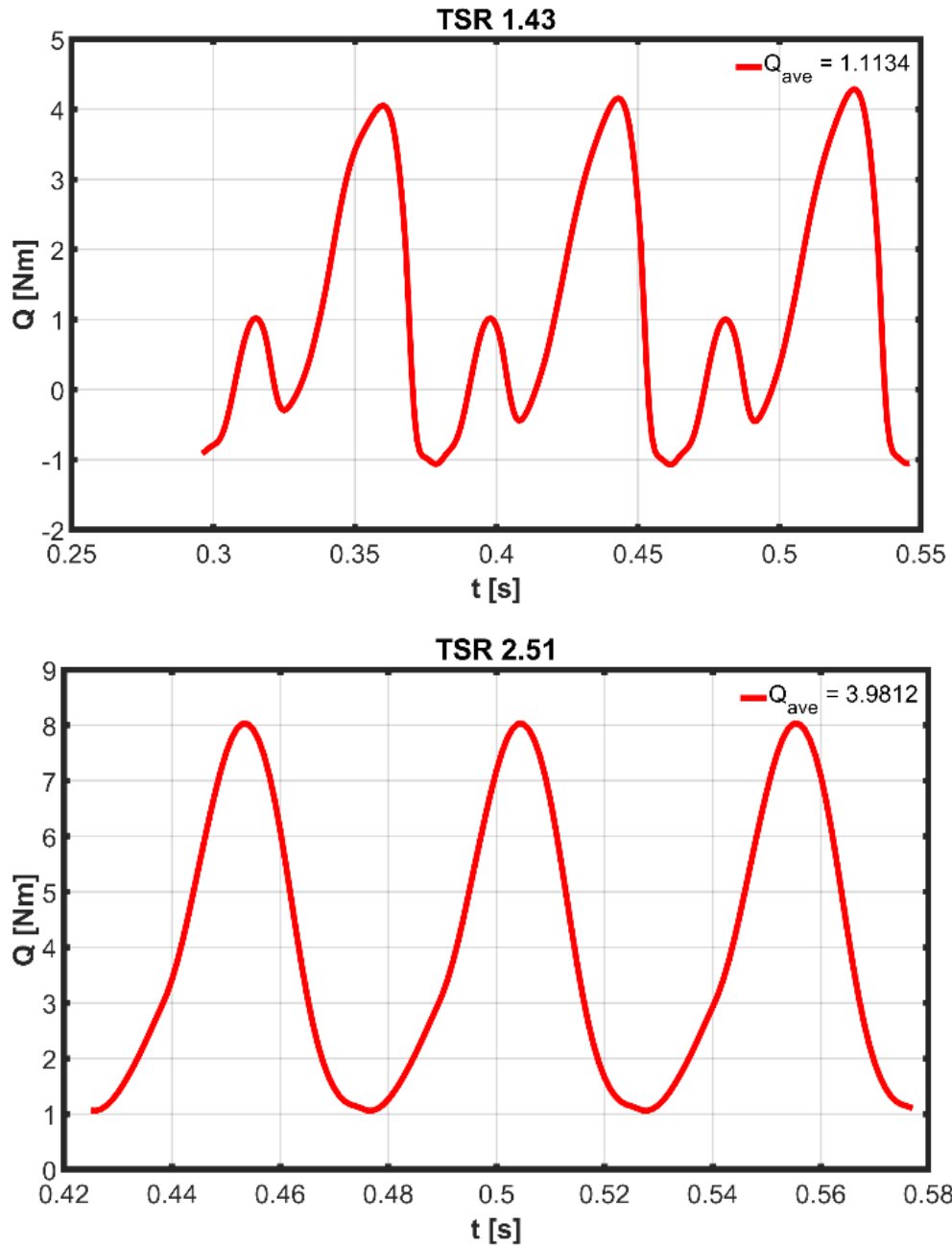
Figure 13. Torque graphs of Design C for TSR 1.43 and 4.00

At a TSR value of 1.43, the minimum torque value is -1, while the maximum value is approximately 4.2, and the average value is 1.113 Nm. At a TSR value of 2.51, the minimum torque value is +1, while the maximum value is approximately 8, and the average value is 3.981 Nm. In the case of a TSR of 1.43, the torque values produced by the inner blades are reflected in the graph with relatively smaller peaks compared to the others. However, this is not observed at higher TSR values. Streamlines graphics have also been generated for Design C, and the flow movement has been interpreted based on these graphics. The streamlines contour obtained at a

TSR value of 2.51 and the given position is shown in Figure 14. The turbulence intensity contours obtained for Design C, specifically for the TSR value of 2.51, are also illustrated in Figure 14.
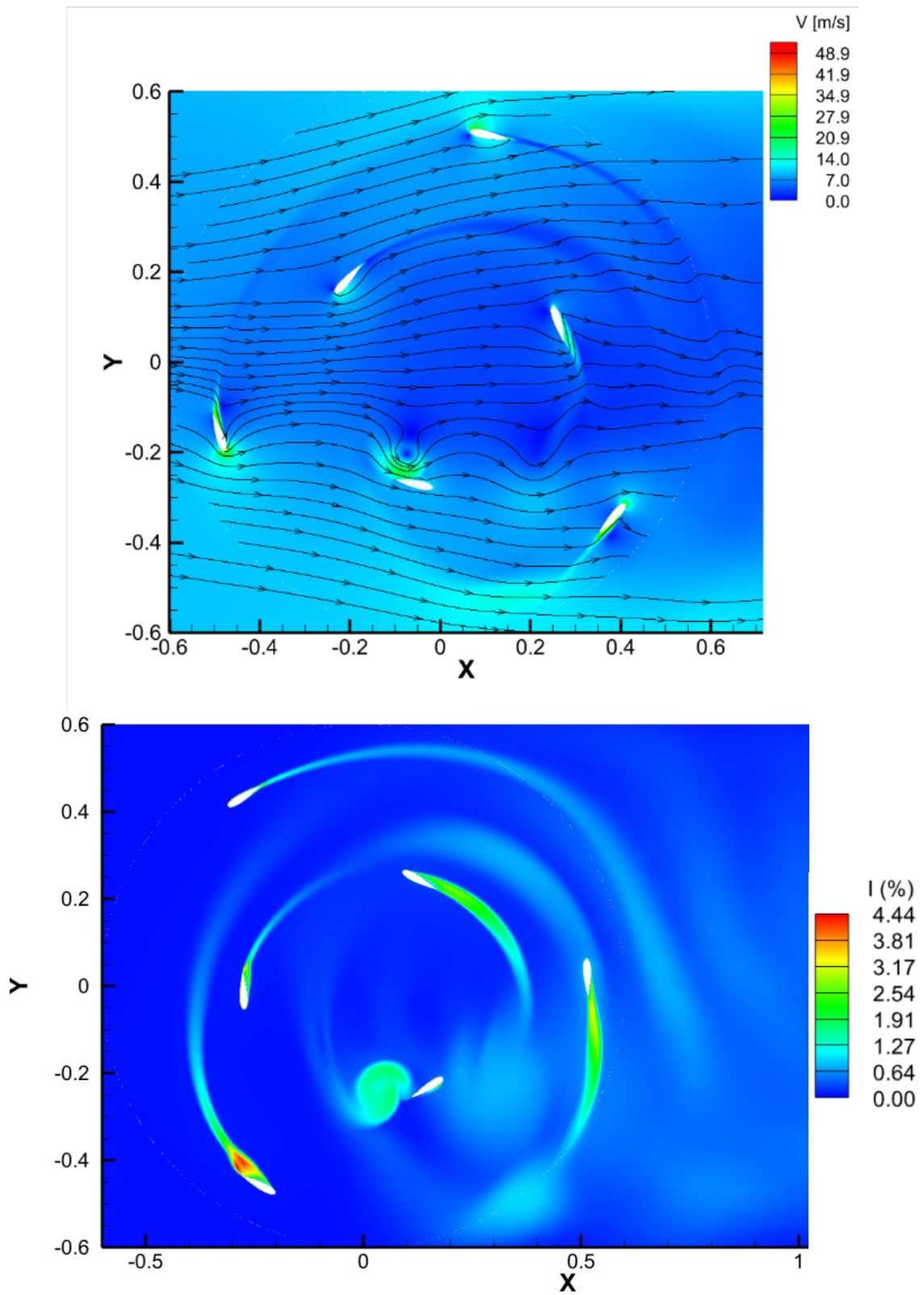

Figure 14. Streamlines and turbulence intensity contours for Design C

When both blades align in the flow direction, it is observed that the inner blade is negatively affected by the wake of the outer blade at the coordinates (x=-0.05, y=-0.2). This is because a vortex has formed on the inner side of the airfoil at this position. Detailed analyses conducted on such contours are important for detecting irregularities in the flow. It has been determined that the maximum value of the turbulence intensity contours obtained at different positions ranges from 4.2% to 5.32%. Looking at the wake obtained for Design C at a TSR of 2.51 unlike Design B, the flow can return to its original state at x=3 m. This also suggests that the distance between the two turbines should be at least three times the diameter of the turbines when they are placed in the wind direction.
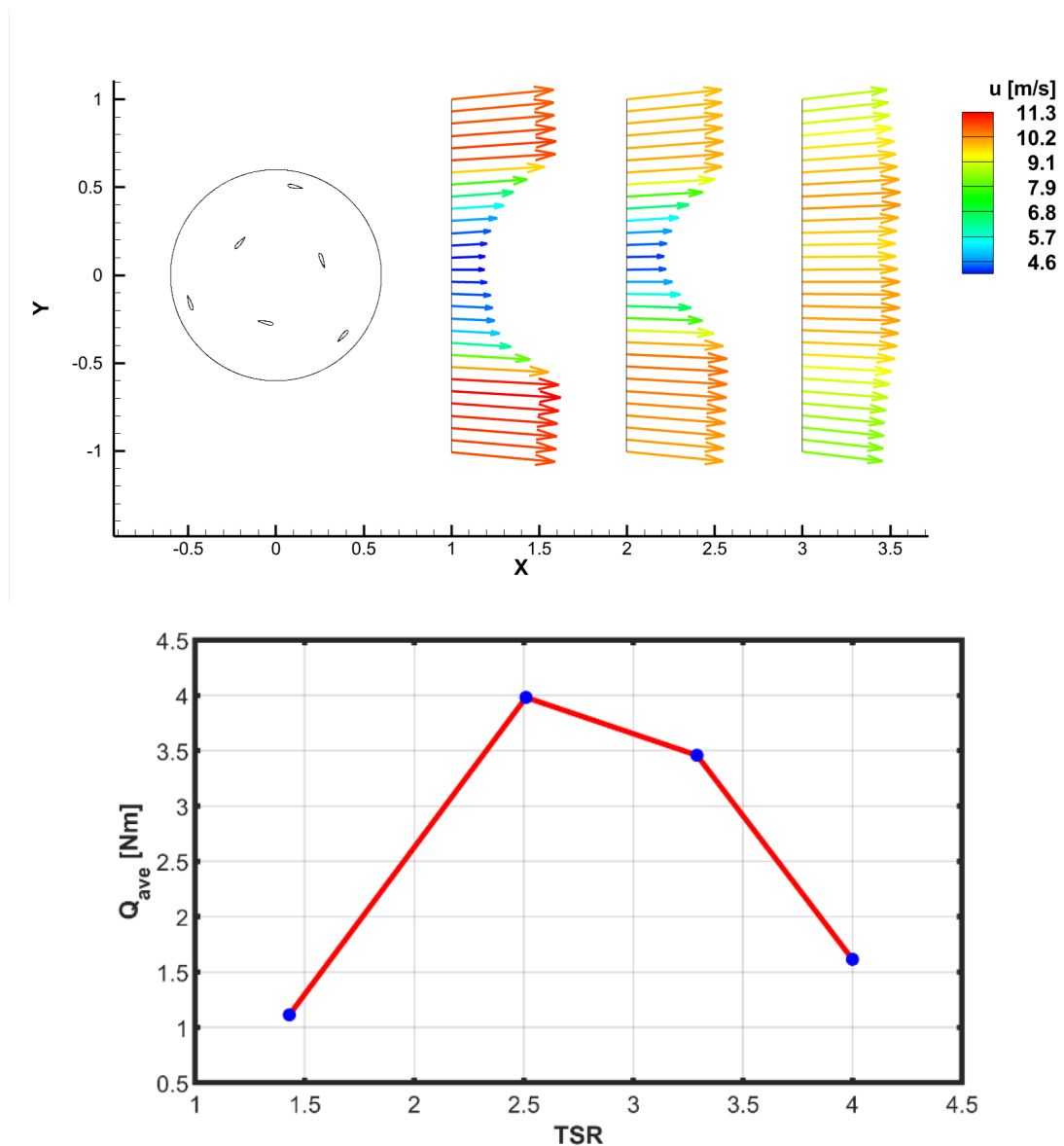

Figure 15. The velocity profiles in the wake flow and average torque values of Design C

The average torque values obtained for Design C at four different TSR values are shown in the figure. When compared to Designs A and B, it is evident that Design C produced better torque at a TSR of 1.43 but generated less torque at higher TSR values.

Design D: Two different hybrid turbines were designed, with a Savonius turbine inside and a Darrieus turbine outside. These were created separately, with different positioning of the Savonius blades relative to the Darrieus blades, and are referred to as Design D and Design E. Two of the *CP* graphs obtained for Design D are shown in Figure 16.
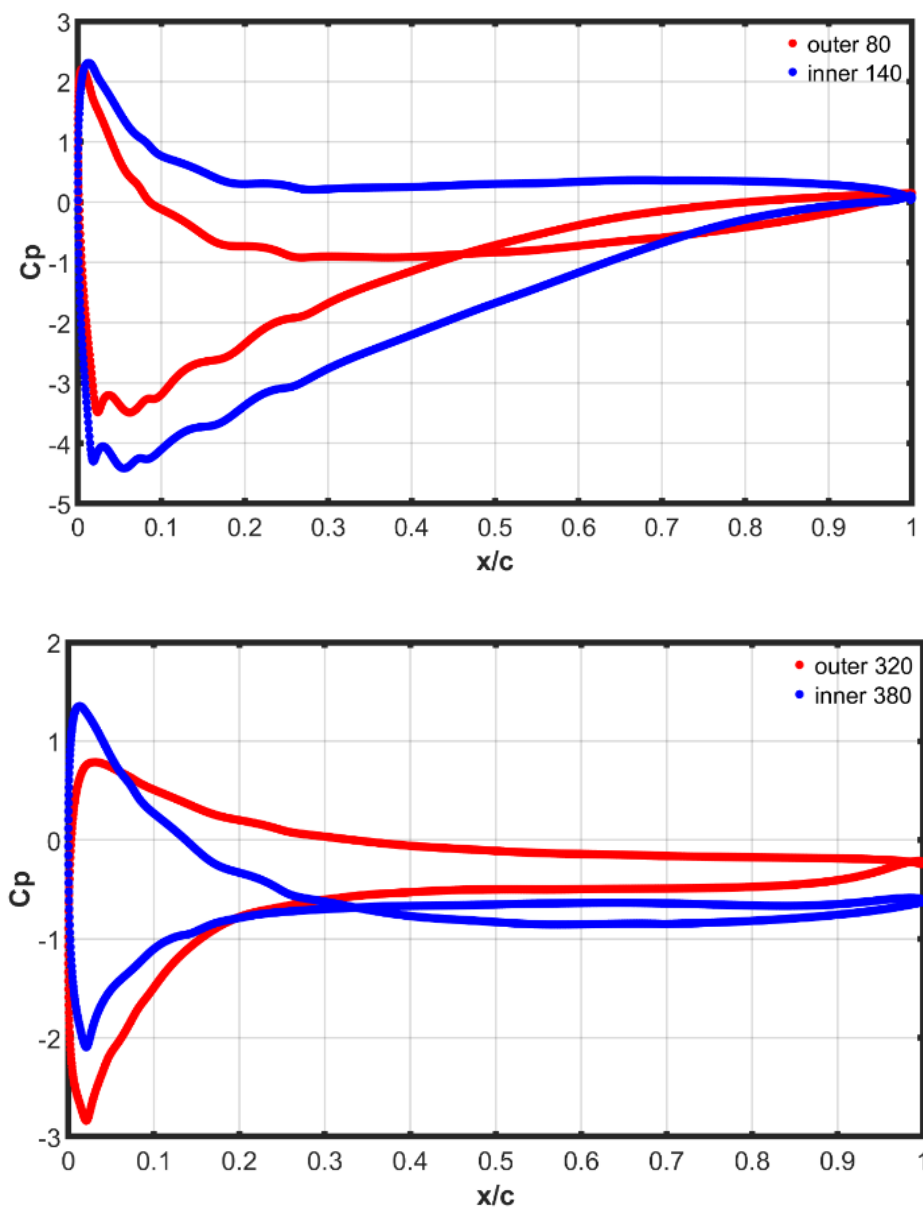

Figure 16. Pressure coefficient (*CP*) graphs of Design D

When examining the graphs obtained at a TSR of 2.51, at the 80° position (relative to the outer blade), the inner blade generates better aerodynamic performance, resulting in higher lift, while at the 320° position, the outer blade performs better. By interpreting the *CP* graphs, which provide information about the pressure distribution on the blade section (airfoil), it is possible to identify positions with weak aerodynamic performance and make design improvements accordingly. The torque-time graphs obtained for Design D at TSR values of 1.43 and 3.29 are provided.
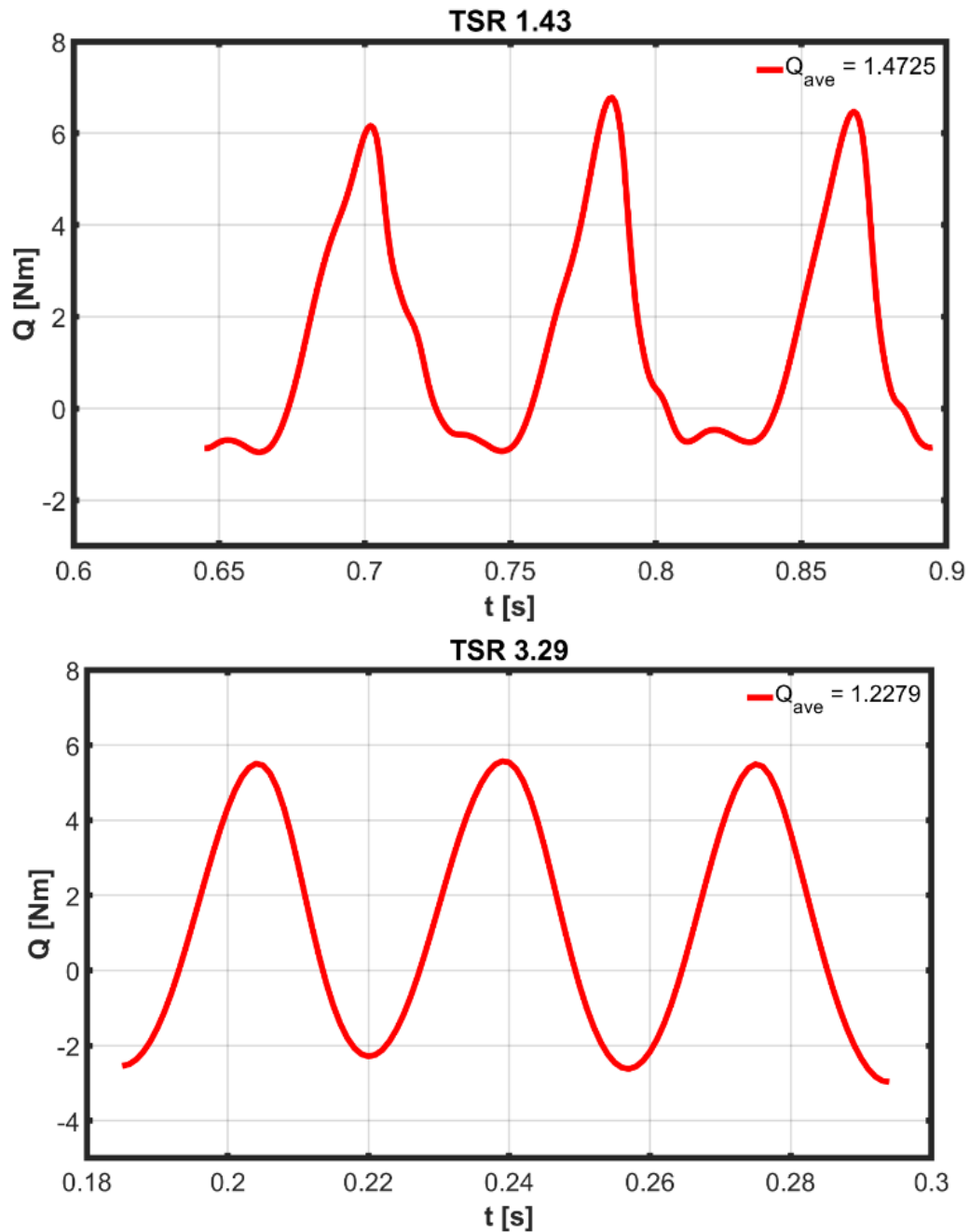
Figure 17. Torque graphs of Design D for TSR 1.43 and 4.00

At low TSR values, the average torque value was 1.473, while at high TSR values, it was 1.223. This indicates a different situation compared to Designs A, B, and C. The influence of the Savonius design is noteworthy. With these results, it has been revealed that Design D produced higher torque than Designs A, B, and C at a TSR of 1.43. Examples of the streamline and turbulence intensity contours are shown in Figure 18.
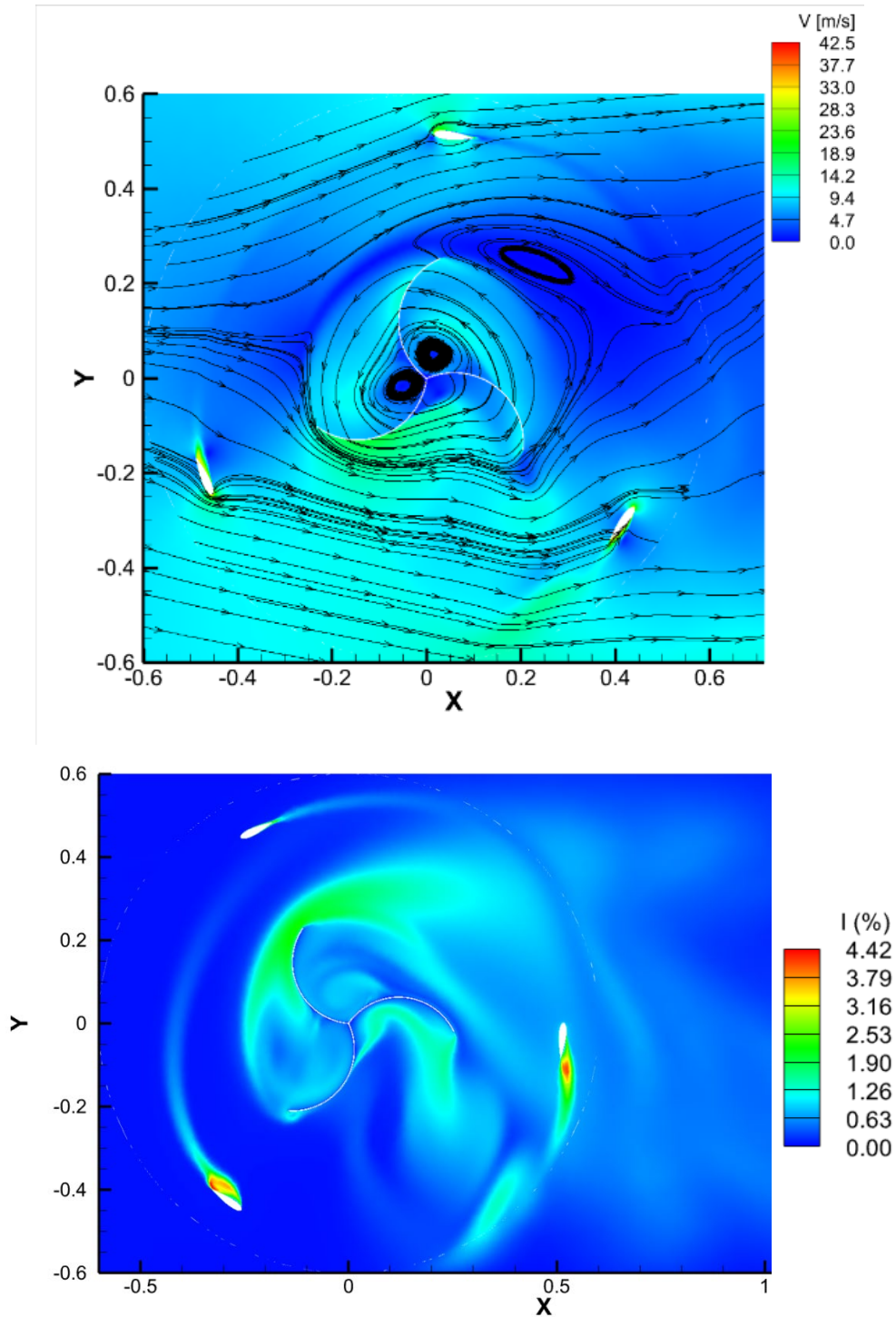
Figure 18. Streamlines and turbulence intensity contours for Design D

In this contour obtained for Design D at a TSR of 2.51, the vortices formed near the centers of the Savonius blades are notable. It is evident from the figure that the distance between the Savonius and Darrieus geometries is sufficient to not significantly disrupt each other's flow patterns. The turbulence intensity values for this design at a TSR of 2.51 have been found to be in the range of 3.44% to 4.42%. Compared to the values in designs A, B, and C, this design has the lowest turbulence intensity value. However, this has not resulted in producing a higher torque value at the specified TSR. Looking at the flow pattern of Design D, it is observed that, like Design B, the flow at the x=3 m position is still affected by the turbine and has not stabilized. The average torque values for Design D, varying according to four different TSR values, are shown in Figure 19.
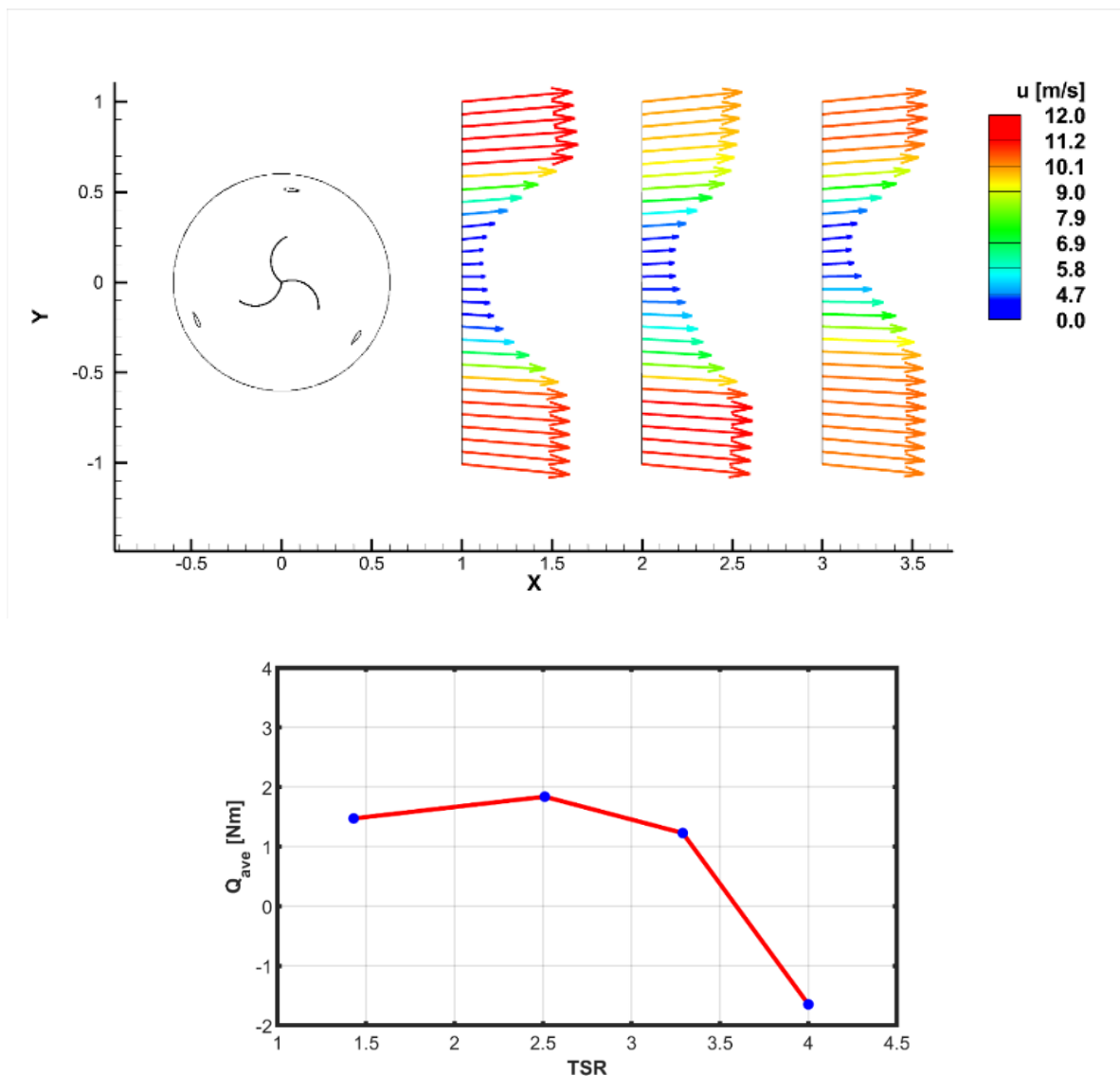
Figure 19. The velocity profiles in the wake flow and average torque values of Design D

Unlike designs A, B, and C, the torque value produced at low TSR values is close to the torque value produced at a TSR of 2.51. Another noteworthy observation is the generation of negative torque at a TSR of 4. This indicates that Design D will be unable to produce torque and, consequently, power beyond approximately a TSR value of 3.5. It can be said that the most efficient TSR range for this turbine would be between 1 and 3, but more specifically narrowed down to between 1.5 and 2.5.

Design E: Two examples of the pressure coefficient (*CP*) graphs obtained from the CFD analyses conducted on Design E are provided in Figure 20.
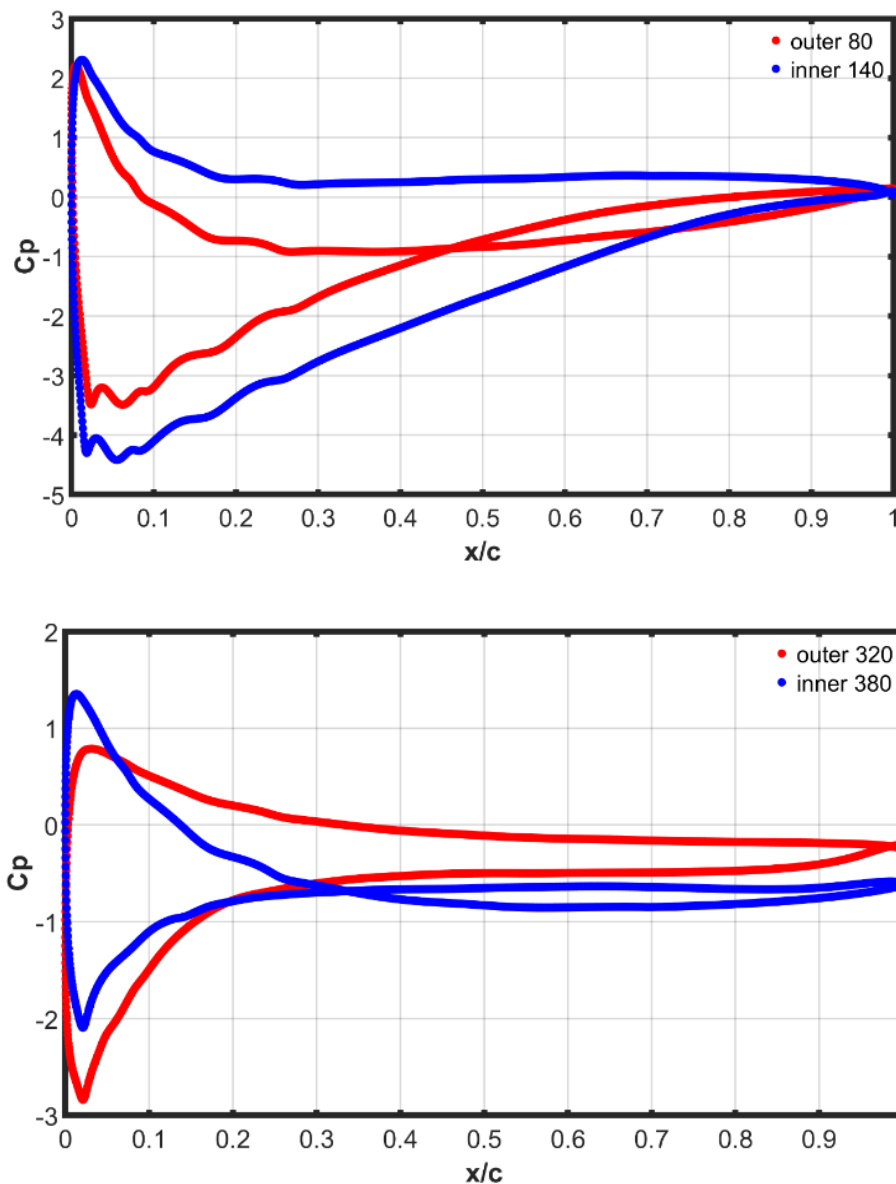
Figure 20. Pressure coefficient (*CP)* graphs of Design E

At a TSR value of 2.52, the Savonius blade produces better thrust with a greater pressure difference at the 80° position (for Darrieus), while the Darrieus blade generates less tangential force at the 140° position. At the 320° position, however, the Darrieus blade produces lift and tangential force with a better pressure difference compared to the Savonius blade. Overall, based on the results obtained, it can be stated that the Savonius design generates higher torque than the Darrieus at low TSR values. Torque-time graphs for Design E at four different TSR values have been obtained, with two examples shown in Figure 21.
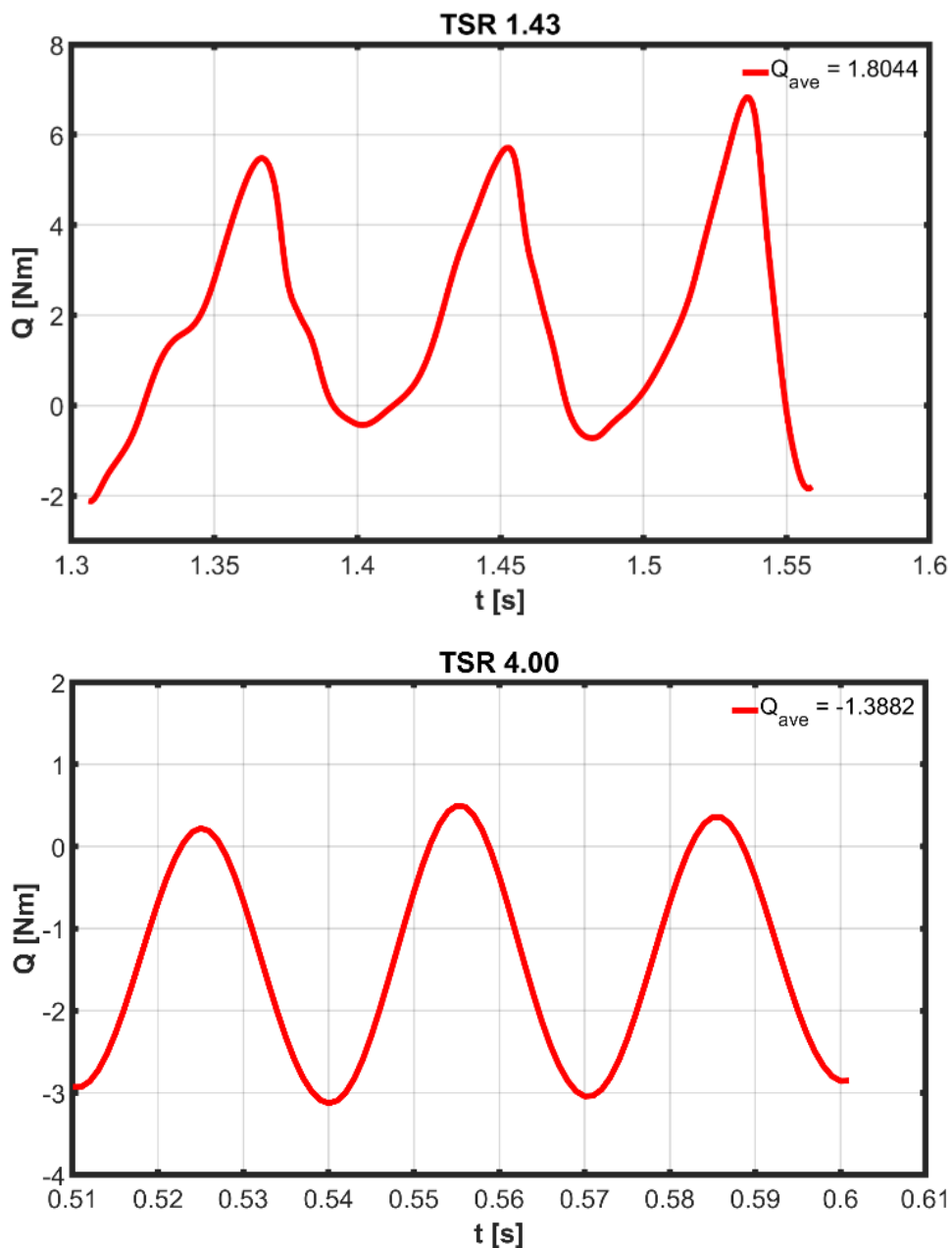

Figure 21. Torque graphs of Design E for TSR 1.43 and 4.00

At a TSR value of 1.43, the maximum, minimum, and average torque values were calculated as 6, -2, and 1.804 Nm, respectively. For a TSR value of 4, these values were found to be 0.2, -3, and -1.388 Nm, respectively. As in Design D, the torque value at TSR 4 is negative here as well, indicating that this design cannot produce torque at this TSR value. One example of the streamlines contours for this design is shown in the figure, obtained at a TSR value of 2.51, just like in all other designs. An example of the contours showing how the turbulence intensity values change in the flow fields of Design E at different TSR values and positions is also provided in Figure 22.
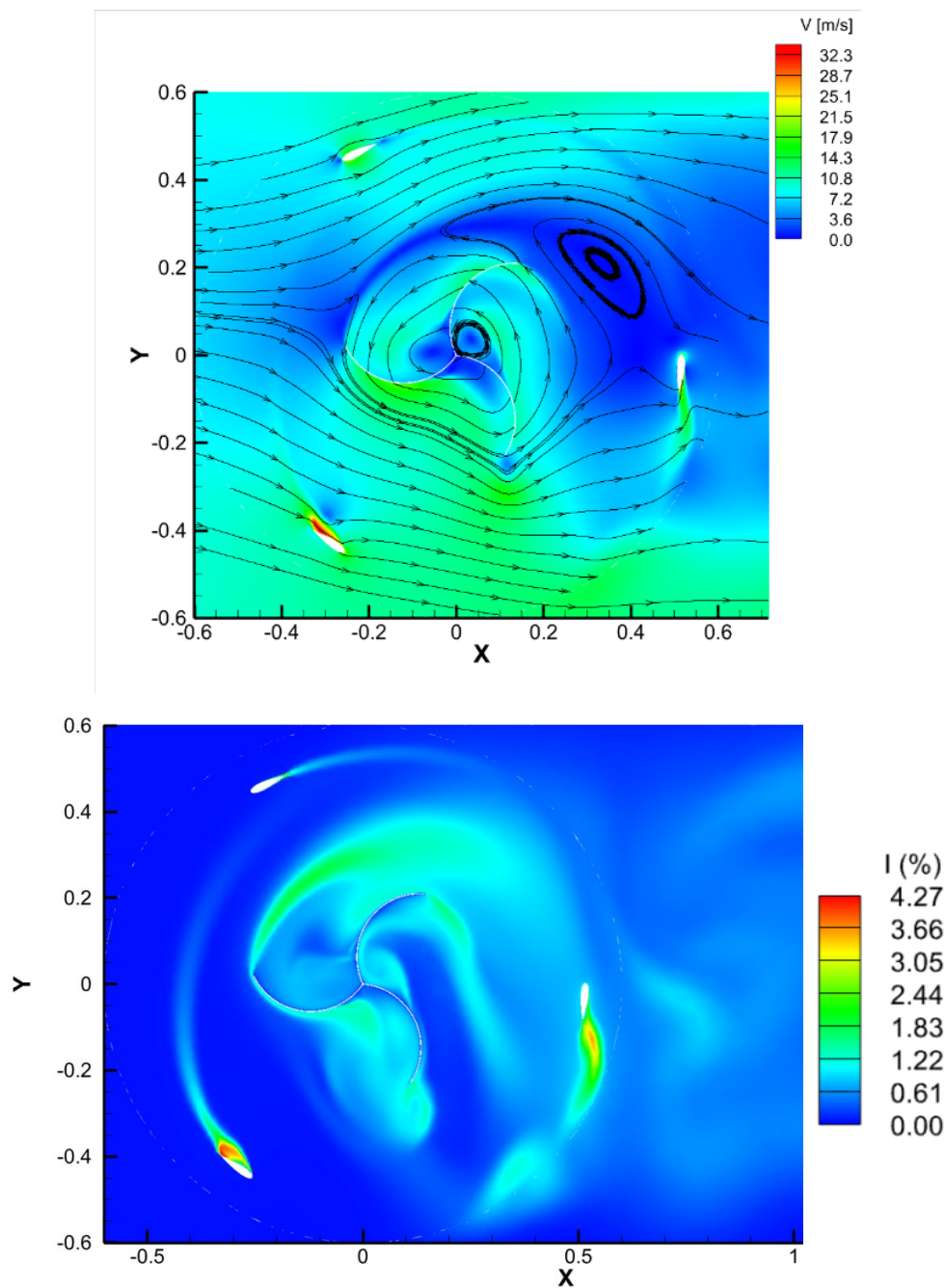
Figure 22. Streamlines and turbulence intensity contours for Design E

In the shown position, vortices caused by the Savonius are observed as black closed curves. It can be easily stated that the Darrieus blades do not create similar vortices. The maximum value of flow velocity obtained for the contour shown is 32.3 m/s; however, this velocity varies at different positions. For TSR 2.51, the maximum velocity values obtained for Designs A, B, C, D, and E are 48.7, 46.4, 48.9, and 42.5 m/s, respectively. These values can vary depending on the TSR, position, and designs. Therefore, a torque performance comparison cannot be made based on these values. The maximum value obtained in this contour is 4.78. When comparing the average turbulence intensity values at different positions for all designs A, B, C, D, and E at TSR 2.51, the highest value occurs in Design A, followed by B, C, E, and D in that order. Looking at the streamlines of Design E shown in Figure 23, we can see that the flow velocity recovers again at x = 3 m.
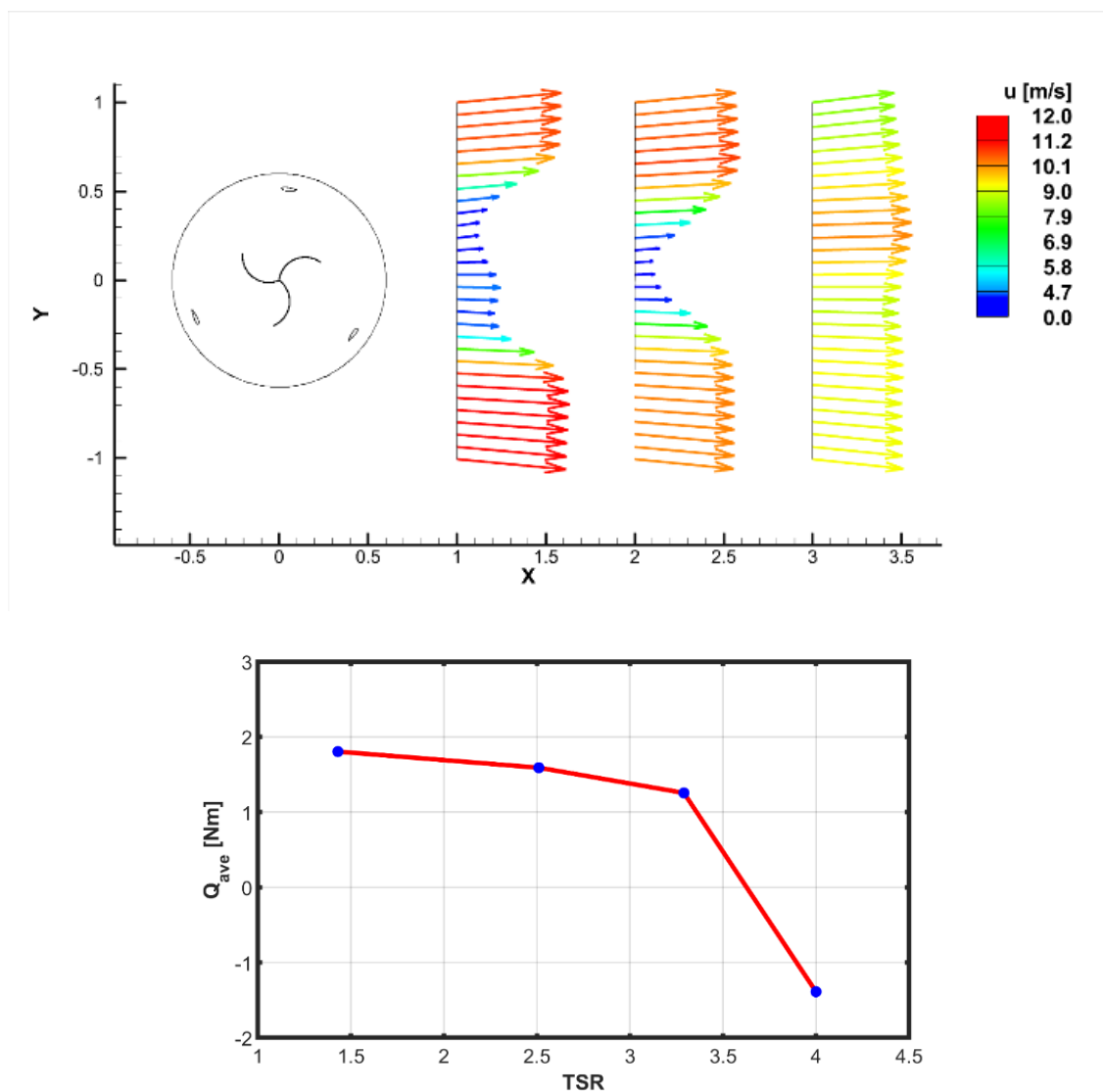

Figure 23. The velocity profiles in the wake flow and average torque values of Design E

As a result of the CFD analyses for this design, the average torque values calculated for TSR values of 1.43, 2.51, 3.29, and 4 are 1.804, 2.591, 1.255, and -1.388 Nm, respectively. Like Design D, Design E could not produce positive torque at a TSR value of 4. The results are presented graphically. At the smallest TSR value of 1.43, the turbine design that produced the highest torque was Design E.

In hybrid turbine designs, visualizing the flow around the Savonius and Darrieus blades helps observe their individual effects on the flow. However, at both low and high speeds, particularly at different azimuth angles, the flow becomes complex. The Savonius blade interferes with the flow reaching the Darrieus blade at the ideal angle of attack. This limits torque and power production at high TSR, making hybrid designs less effective than standart Darrieus turbines. Savonius turbines operate with drag at low speeds, while Darrieus turbines generate lift at higher speeds, making hybrid turbines more efficient across a range of speeds.

In this present study, the graphs comparing C_P values of five different designs at four TSR values are presented in Figure 24.
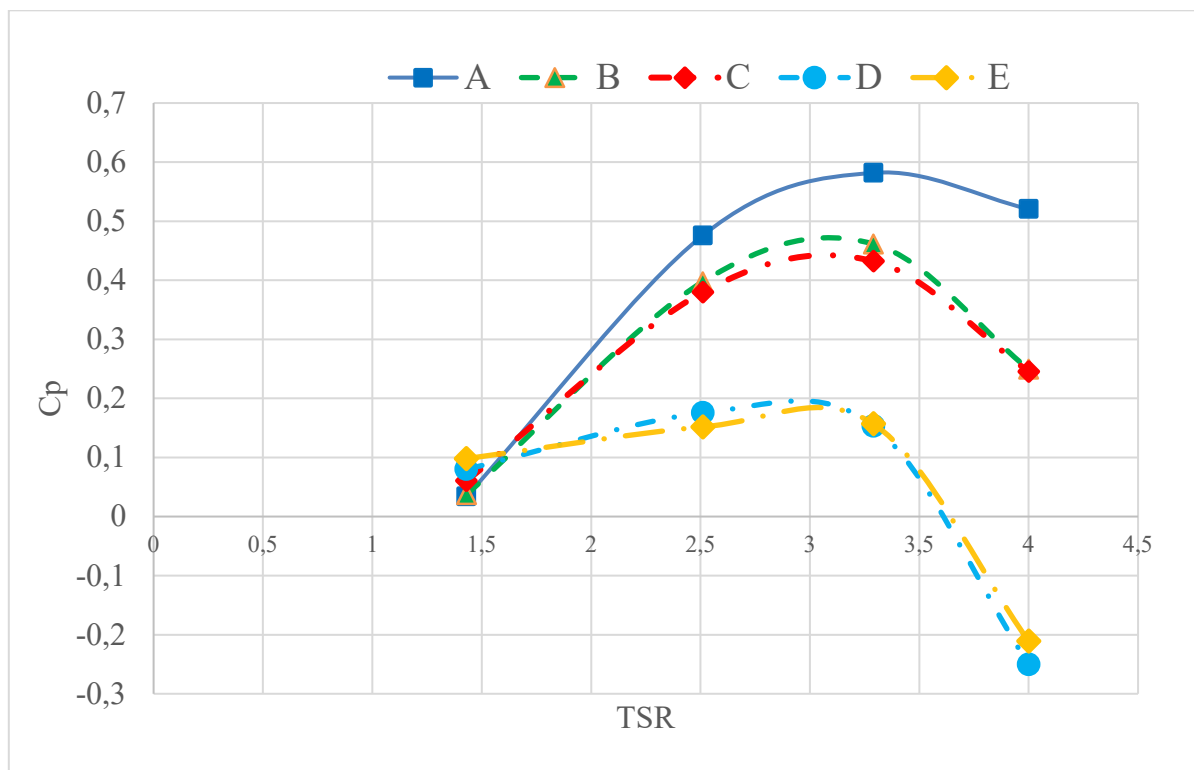

Figure 24. C_P-TSR Graphs of Five Different Designs

At TSR values below 1.5, hybrid designs exhibit better power factor values [4]. In this present CFD study, the average torque values calculated for designs A, B, C, D, and E at four different TSR values are summarized in Table 2.

Table 2. Average Torque values (Nm) of five different designs (Design A, B, C, D, E)

TSR	A	B	C	D	E
1.43	0.629	0.681	1.113	1.473	1.804
2.51	4.988	4.166	3.980	1.838	1.591
3.29	4.654	3.692	3.458	1.228	1.255
4	3.425	1.640	1.615	-1.646	-1.388

In this present CFD study, the comparison of the average torque values calculated for designs A, B, C, D, and E at four different TSR values is summarized in Figure 25.
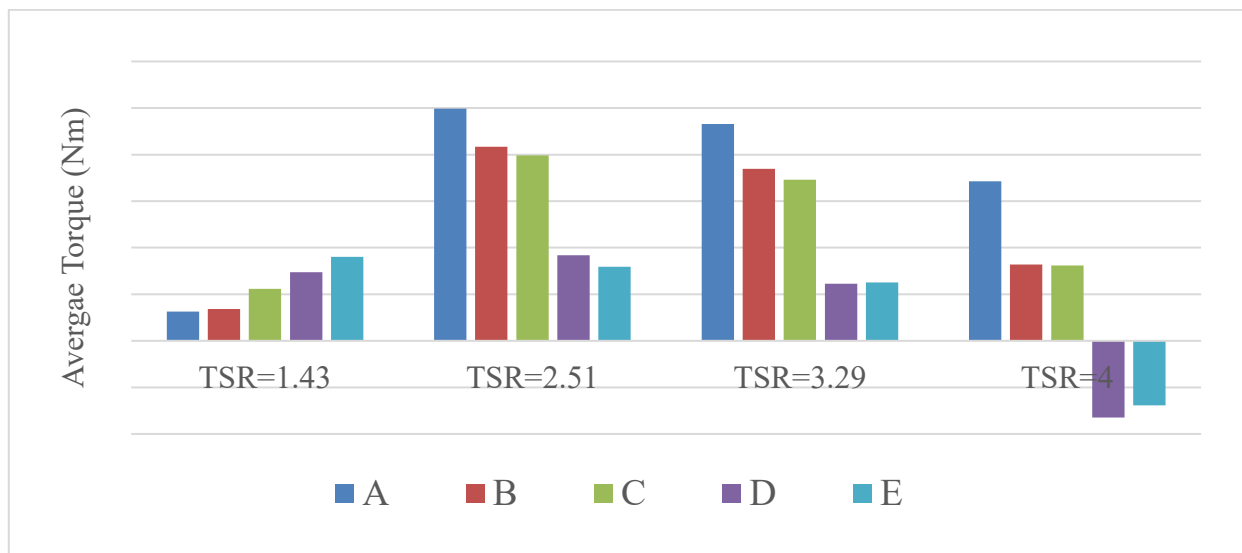
Figure 25. Comparing average torque values of five designs at four different TSR values

The hybrid designs do not reach the standard Darrieus power coefficient values. The nested two Darrieus hybrid design produces higher torque values compared to the standard Darrieus at low TSR values. The outer Darrieus and inner Savonius hybrid design produces better torque at low TSR values compared to the double Darrieus design but generates significantly less torque at high TSR values compared to the double Darrieus.

The contribution of this study to the literature is the detailed investigation of the performance of hybrid Savonius-Darrieus turbines through 2D CFD analyses at different TSR, highlighting the

effects of wake profiles and adverse flow conditions on torque and power generation. While Savonius and Darrieus turbines have been studied individually or in hybrid forms in the literature, this study systematically compares different hybrid designs (standard Darrieus, double Darrieus, and Savonius-Darrieus) for the first time. Although the torque advantage of hybrid turbines at low speeds has been discussed in the literature, the connection between power generation, wake analysis, and torque has not been addressed in such a comprehensive manner, making this study unique. Furthermore, the effects of flow disturbances in the wake on the torque production of hybrid turbines are elaborated in this study, providing significant insights for optimized designs. In this context, the results obtained indicate that hybrid turbines offer advantages at low speeds but also highlight areas for improvement in terms of power generation.

It can be stated that the values obtained in this present study are consistent with the results presented in the literature. Sun et al. [22] investigated the effect of the installation position of the Savonius blade and observed that C_P of the hybrid vertical axis wind turbine (VAWT) was lower than that of the Darrieus rotor used alone. The hybrid VAWT can start operating as efficiently as the Savonius rotor alone, but it has a lower C_P than the Darrieus rotor used alone. This result is consistent with the literature as [5, 11, 19]. Here, C_P values of the Standard Darrieus turbine (Design A) obtained through CFD in this study were compared with the results of Castelli's CFD and experimental findings [20] and those from four other studies in the literature [4, 22, 23, 24]. This comparison of C_P and instantenous torque coefficiet (C_Q) values are shown in Figure 26 and Figure 27.

The compatibility of the results obtained in this study with the results from the literature [4, 20, 22, 23, 24] can be interpreted from the graphs provided. This current study has the same dimensions as the Castelli study [20], but while Castelli's CFD study is three-dimensional, our study is two-dimensional. Although the designs in the other studies are quite similar, the dimensions are different.

As a result of the CFD analyses conducted in this study, it has been determined that the standard Darrieus has a higher C_P value over a wide range of TSR values compared to all other designs, as also shown in the literature, Figure 28 [4].
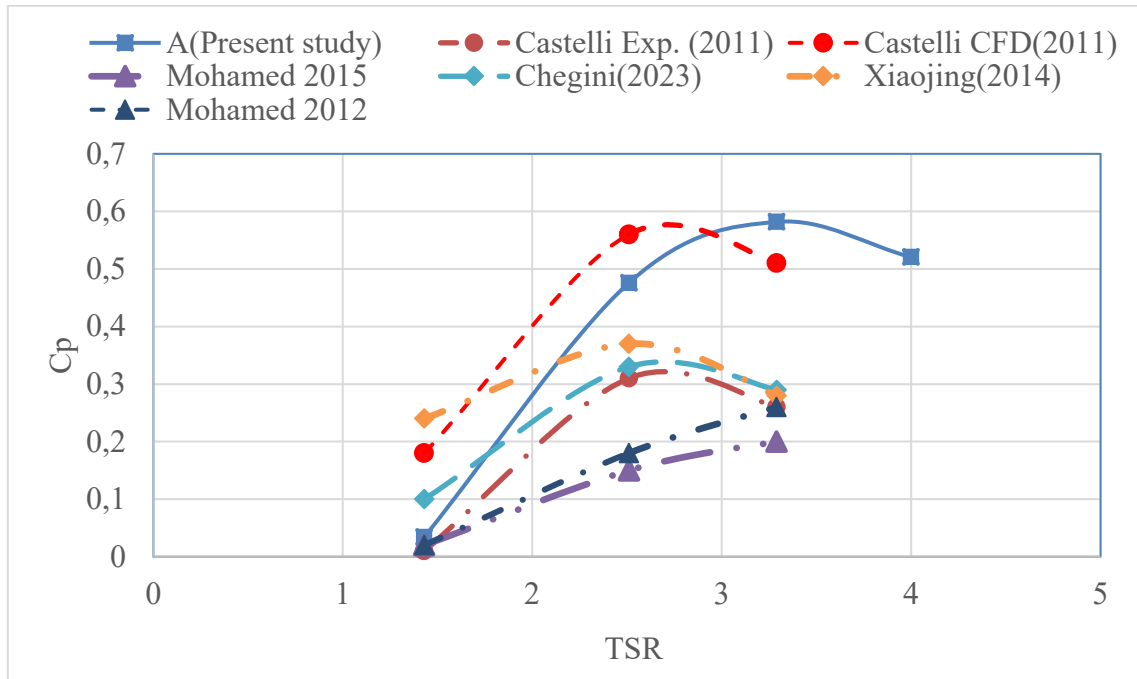
Figure 26. Comparing Cp results standart darrieus (Design A) to the literature[4, 20, 23, 24]
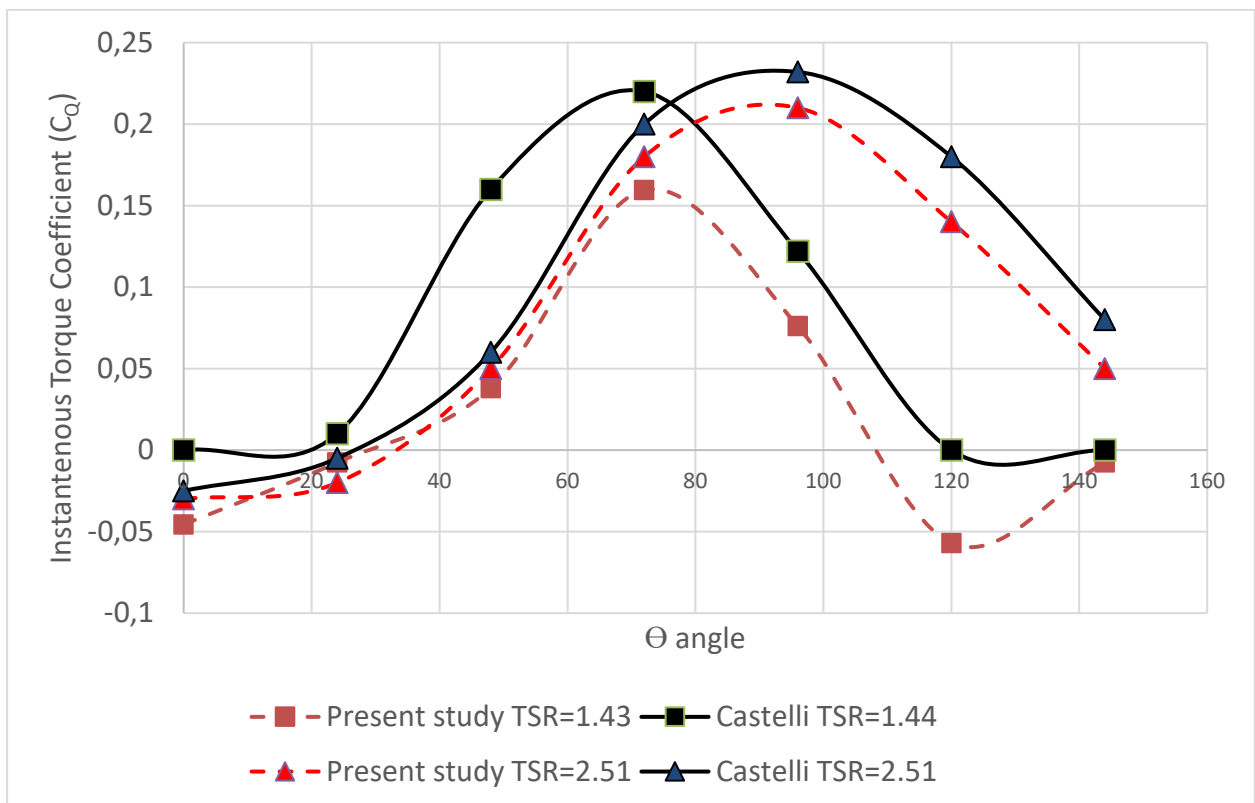
Figure 27. Comparing C_Q for single blade of standart darrieus (Design A) to the literature[20]
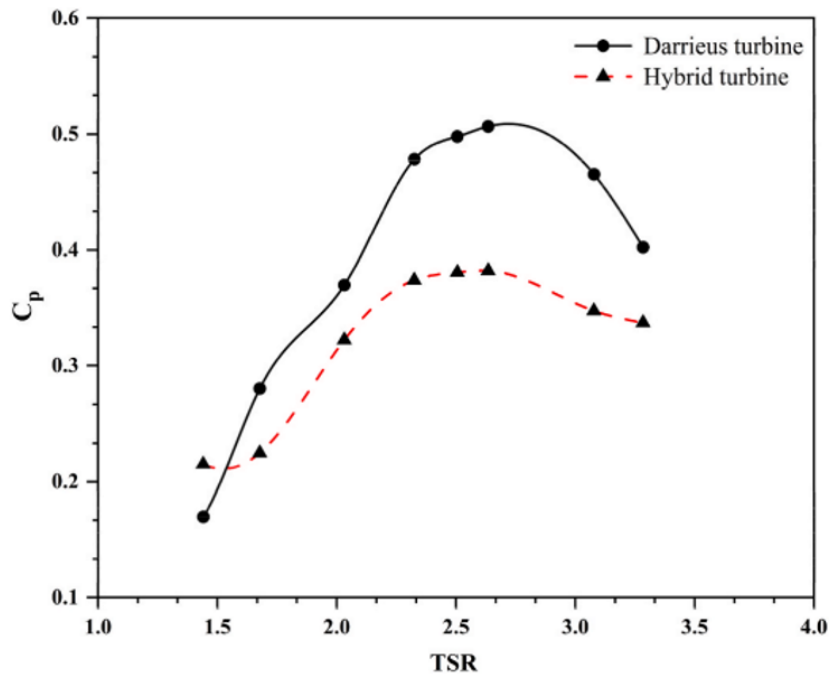
Figure 28. Comparing C_P values versus TSR values for Darrieus and Hybrid designs [4]

4. CONCLUSION

The study presents five different wind turbine designs, including a standard Darrieus turbine, two nested Darrieus hybrids, and two Darrieus-Savonius hybrids. Two-dimensional unsteady CFD analyses have been performed on these turbines. The changes in torque values over time are presented graphically, and the flow characteristics, turbulence intensity, and wake flow have been analyzed. As a result, it has been determined that hybrid designs, while not producing as much power as the standard Darrieus turbine, provide higher torque at low TSR with the nested Darrieus design. The Darrieus-Savonius hybrid produces better torque than the double Darrieus design at low TSR but its performance decreases at high TSR.

This study shows that the presented hybrid turbines provide advantages at low tip speed ratios but need improvements in terms of power production. Incorporating three-dimensional analyses and experimental validations in future studies is crucial for better understanding the real-world performance of these designs. Many parameters, such as Darrieus airfoil selection, different size ratios, various values of Savonius blade pitch angles, the use of flow-directing apparatuses, and different numbers of blades, can be considered to enhance the performance of hybrid designs at low wind speeds. To find the best configurations, different optimization methods like Response Surface Methodology (RSM), Particle Swarm Optimization (PSO), and Genetic Algorithms can

be applied. These techniques help navigate the complex landscape of design variables—such as blade shape, radius, and angle—to achieve optimal performance across a range of scenarios. By using user-defined functions (UDFs) in CFD analyses, the effects of wind speed changes over time or with height on performance can be examined. This could allow for the simulation of more complex flow conditions. These studies can initially be conducted using CFD, and the designs that perform better can be prototyped and validated through experimental measurements to improve the reliability of the results. Compared to standalone Darrieus or Savonius turbines, the hybrid design has more complex flow characteristics, making predictions challenging with conventional theorems like BEM (Blade Element Momentum) or DMST (Double-Multiple Streamtube). New theoretical models are needed to analyze hybrid aerodynamics effectively.

NOMENCLATURE

P_{max}	The wind power (W)	R	Radius (m)
ρ	The air density (kg/m^3)	C_Q	Instantenous torque coefficient
D	The diameter of the turbine (m)	ω	Rotational speed (rad/s)
H	The height of the turbine (m)	N	Revolution number per minutes
c	Chord length (m)	CP	Pressure coefficient
A	The turbine swept area (m^2)	TSR	Tip speed ratio
V	The wind velocity (m/s)	VAWT	Vertical axis wind turbine
C_P	The power coefficient	HAWT	Horizontal axis wind turbine
P_a	Available power (W)	CFD	Computational fluid dynamics
Q	Torque (Nm)	RANS	Reynolds averaged Navies Stokes

DECLARATION OF ETHICAL STANDARDS

The author of the paper submitted declares that there is nothing necessary for achieving the paper that requires ethical committee and/or legal-special permissions.

CONTRIBUTION OF THE AUTHORS

Mehmet Bakırcı: Conducted CFD simulations, performed result analysis, and contributed to the writing of the manuscript.

CONFLICT OF INTEREST

There is no conflict of interest in this study.

REFERENCES

[1] Liu J, Lin H, Zhang J. Review on the technical perspectives and commercial viability of vertical axis wind turbines. Ocean Engineering 2019; 182: 608-626.

[2] Ghosh A, Biswas A, Sharma KK, Gupta R. Computational analysis of flow physics of a combined three bladed Darrieus-Savonius wind rotor. Journal of the Energy Institute 2015; 88(4): 425-437.

[3] Pan J, Ferreira C, Van Zuijlen A. Performance analysis of an idealized Darrieus–Savonius combined vertical axis wind turbine. Wind Energy 2024; 27(6): 612-627.

[4] Chegini S, Asadbeigi M, Ghafoorian F, Mehrpooya M. An investigation into the self-starting of Darrieus-Savonius hybrid wind turbine and performance enhancement through innovative deflectors: A CFD approach. Ocean Engineering 2023; 287: 115910.

[5] Pallotta A, Pietrogiacomi D, Romano G P. Hybrid—a combined Savonius-Darrieus wind turbine: performances and flow fields. Energy 2020; 191: 116433.

[6] Morshed KN, Rahman M, Molina G, Ahmed M. Wind tunnel testing and numerical simulation on aerodynamic performance of a three bladed Savonius wind turbine. International Journal of Energy and Environmental Engineering (IJEEE) 2013; 4(18).

[7] Mohamed HM, Alqurashi F, Thévenin D. Performance enhancement of a Savonius turbine under effect of frontal guiding plates. Energy Reports 2021; 7: 6069-6076.

[8] Chen J, Yang H, Yang M, Xu H. The effect of the opening ratio and location on the performance of a novel vertical axis Darrieus turbine. Energy 2015; 89: 819-834.

[9] Sun SY, Liu H J, Peng H Y. Power performance and self-starting features of H-rotor and helical vertical axis wind turbines with different airfoils in turbulence. Energy Conversion and Management 2023; 292: 117405.

[10] Qamar SB, Janajreh I. A comprehensive analysis of solidity for cambered Darrieus VAWTs. International Journal of Hydrogen Energy 2017; 42: 19420-19431.

[11] Liang X, Fu S, Ou B, Wu C, Chao CYH, Pi K. A computational study of the effects of the radius ratio and attachment angle on the performance of a Darrieus–Savonius combined wind turbine. Renewable Energy 2017; 113: 329-334.

[12] Li Q, Maeda T, Kamada Y, Murata J, Shimizu K, Ogasawara T, Nakai A, Kasuya T. Effect of solidity on aerodynamic forces around straight-bladed vertical axis wind turbine by wind tunnel experiments (depending on number of blades). Renewable Energy 2016; 96: 928-939.

[13] Li L, Chopra I, Zhu W, Yu M. Performance analysis and optimization of a vertical-axis wind turbine with a high tip-speed ratio. Energies 2021; 14(996).

[14] Zamani M, Maghrebi MJ, Varedi SR. Starting torque improvement using J-shaped straight-bladed Darrieus vertical axis wind turbine by means of numerical simulation. Renewable Energy 2016; 95: 109-126.

[15] Acarer S. Peak lift-to-drag ratio enhancement of the DU12W262 airfoil by passive flow control and its impact on horizontal and vertical axis wind turbines. Energy 2020; 201: 117659.

[16] Jain S, Saha UK. The state-of-the-art technology of H-type Darrieus wind turbine rotors. Journal of Energy Resources Technology 2020; 142: 1-25.

[17] Ahmad M, Shahzad A, Akram F, Shah SIA. Design optimization of Double-Darrieus hybrid vertical axis wind turbine. Ocean Engineering 2022; 287: 115910.

[18] Gavalda J, Massons J, Diaz F. Experimental study on a self-adapting Darrieus-Savonius wind machine. Solar and Wind Techonology 1990; 7(4): 457-461.

[19] Sun X, Chen Y, Cao Y, Wu G, Zheng Z, Huang D. Research on the aerodynamic characteristics of a lift-drag hybrid vertical axis wind turbine. Advances in Mechanical Engineering 2016; 8: 1-11.

[20] Castelli MR, Englaro A, Benini E. The Darrieus wind turbine: proposal for a new performance prediction model based on CFD. Energy 2011; 36(8): 4919-4934.

[21] Fertahi SeD, Belhadad T, Kanna A, Samaouali A, Kadiri I, Benini E. A critical review of CFD modeling approaches for Darrieus turbines: Assessing discrepancies in power coefficient estimation and wake vortex development. Fluids 2023; 8(242).

[22] Sun X, Wang Y, An Q, Cao Y, Wu G, Huang D. Aerodynamic performance and characteristic of vortex structures for Darrieus wind turbine. Journal of Renewable and Sustainable Energy 2014; 6.

[23] Mohamed M. Performance investigation of H-rotor Darrieus turbine with new airfoil shapes. Energy 2012; 47: 522-530.

[24] Mohamed M, Ali A, Hafiz A. CFD analysis for H-rotor Darrieus turbine as a low-speed wind energy converter. Engineering Science and Technology 2015; 18: 1-13.

[25] Gupta R, Biswas A, Sharma KK. Comparative study of a three-bucket Savonius rotor with a combined three-bucket Savonius–three-bladed Darrieus rotor. Renewable Energy 2008; 33: 1974–1981.

[26] Tian W, Mao Z, Zhang B, Yanjun Li. Shape optimization of a Savonius wind rotor with different convex and concave sides. Renewable Energy 2018; 117: 287-299.

[27] Abdelaziz KR , Nawar MAA, Ramadan A, Attai YA, Mohamed MH. Performance investigation of a Savonius rotor by varying the blade arc angles. Ocean Engineering 2022; 260: 112054.